Electronic Supplementary Material (ESI) for ChemComm.
This journal is © The Royal Society of Chemistry 2022

Electronic Supplementary Information

Ion-pairing assemblies of heteroporphyrin-based π-electronic cation with various counteranions

Masaki Fujita, Yohei Haketa, Hiroki Tanaka, Nobuhiro Yasuda and Hiromitsu Maeda*

Department of Applied Chemistry, College of Life Sciences, Ritsumeikan University, Kusatsu 525–8577, Japan, Fax: +81 77 561 2659; Tel: +81 77 561 5969; E-mail: maedahir@ph.ritsumei.ac.jp and Diffraction and Scattering Division, Japan Synchrotron Radiation Research Institute, Sayo 679–5198, Japan

Table of Contents

1. Synthetic procedures and spectroscopic data

General procedures. Starting materials were purchased from FUJIFILM Wako Pure Chemical Industries Ltd., Nacalai Tesque Inc., Tokyo Chemical Industry Co., Ltd., and Sigma-Aldrich Co., and were used without further purification unless otherwise stated. 5,10,15,20-Tetraphenyl-21-thiaporphyrin **1**[S1] and the Ni^{II} complex **1ni**$^+$ as a Cl^- ion pair (**1ni**$^+$-Cl^-)[S2] were prepared according to the literature procedures. NMR spectra used in the characterization of products were recorded on a JEOL ECA-600 600 MHz spectrometer. All NMR spectra were referenced to solvent. UV-visible spectra were recorded on a Hitachi U-3500 spectrometer. High-resolution (HR) electrospray ionization mass spectrometry (ESI-MS) was recorded on a BRUKER microTOF using ESI-TOF method. Matrix-assisted laser desorption ionization time-of-flight mass spectrometry (MALDI-TOF-MS) was recorded on a Shimadzu Axima-CFRplus. TLC analyses were carried out on aluminum sheets coated with silica gel 60 (Merck 5554). Column chromatography was performed on Sumitomo alumina KCG-1525 and Wakogel C-300.

Ni^{II} complex of 5,10,15,20-tetraphenyl-21-thiaporphyrin as a BF_4^- ion pair, 1ni$^+$-BF_4^-. To a MeOH solution (3 mL) of **1ni**$^+$-Cl^- (28.0 mg, 38.6 μmol) was added $AgBF_4$ (13.0 mg, 66.8 μmol), and the reaction mixture was stirred at r.t. for 15 min, followed by filtration and evaporation to dryness. The residue was purified by silica gel column chromatography (Wakogel C-300; eluent: 5% MeOH/CH_2Cl_2) and was recrystallized from CH_2Cl_2/*n*-hexane to afford **1ni**$^+$-BF_4^- (13.12 mg, 16.9 μmol, 44%) as a brown solid. R_f = 0.17 (5% MeOH/CH_2Cl_2). The signals in ^{1}H NMR (600 MHz, $CDCl_3$, 20 °C), observed at 9.75, 7.49, 7.47, 7.46, and 6.05 ppm, were too broad to discuss in detail due to the paramagnetic Ni^{II}, whereas the signals in $^{13}C\{^1H\}$ NMR (151 MHz, $CDCl_3$, 20 °C) were not detected. UV/vis (CH_2Cl_2, λ_{max}[nm] (ε, 10^5 $M^{-1}cm^{-1}$)): 289 (0.21), 347 (0.17), 432 (0.89), 530 (0.090), 700 (0.027). HRMS (ESI-TOF) *m/z*: [M – BF_4]$^+$ Calcd for $C_{44}H_{28}N_3SNi$ 688.1352; Found 688.1352. MALDI-TOF-MS: *m/z* (% intensity): (negative) 87.0 (100). Calcd for BF_4: ([M – $C_{44}H_{28}N_3SNi$]$^-$): 87.00.

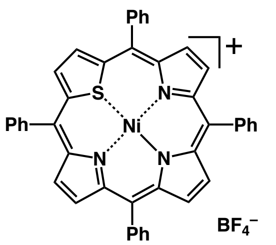

Ni^{II} complex of 5,10,15,20-tetraphenyl-21-thiaporphyrin as a PF_6^- ion pair, 1ni$^+$-PF_6^-. To a MeOH solution (3 mL) of **1ni**$^+$-Cl^- (28.9 mg, 40.0 μmol) was added $AgPF_6$ (20.2 mg, 79.9 μmol) and the reaction mixture was stirred at r.t. for 15 min, followed by filtration and evaporation to dryness. The residue was purified by silica gel column chromatography (Wakogel C-300; eluent: 5% MeOH/CH_2Cl_2) and was recrystallized from CH_2Cl_2/*n*-hexane to afford **1ni**$^+$-PF_6^- (22.3 mg, 26.7 μmol, 67%) as a brown solid. R_f = 0.33 (5% MeOH/CH_2Cl_2). The signals in ^{1}H NMR (600 MHz, $CDCl_3$, 20 °C), observed at 9.96 (s, 2H, β-CH), 9.04–8.89 (β-CH), 8.24 (d, 4H, Ph-H), 8.09 (d, 4H, Ph-H), and 7.93–7.79 (m, 4H, Ph-H) ppm, were too broad to discuss in detail, whereas the signals in $^{13}C\{^1H\}$ NMR (151 MHz, $CDCl_3$, 20 °C) were not fully detected. UV/vis (CH_2Cl_2, λ_{max}[nm] (ε, 10^5 $M^{-1}cm^{-1}$)): 289 (0.22), 347 (0.20), 432 (0.88), 554 (0.095), 688 (0.029). HRMS (ESI-TOF) *m/z*: [M – F_6P]$^+$ Calcd for $C_{44}H_{28}N_3SNi$ 688.1352; Found 688.1352. [M – $C_{44}H_{28}N_3SNi$]$^-$ Calcd for F_6P 144.9647; Found 144.9647. This compound was further characterized by single-crystal X-ray analysis.

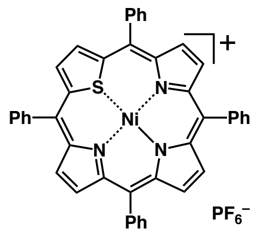

Ni^{II} complex of 5,10,15,20-tetraphenyl-21-thiaporphyrin as a $B(C_6F_5)_4^-$ ion pair, 1ni$^+$-$B(C_6F_5)_4^-$. To a MeOH solution (10 mL) of **1ni**$^+$-Cl^- (31.7 mg, 43.7 μmol) was added Li^+ salt of tetrakis(pentafluorophenyl)borate ($LiB(C_6F_5)_4$) (30.5 mg, 44.5 μmol) and the reaction mixture was stirred at r.t. for 1 h, followed by filtration and evaporation to dryness. The residue was purified by silica gel column chromatography (Wakogel C-300; eluent: 5% MeOH/CH_2Cl_2) and was recrystallized from acetone/*n*-hexane to afford **1ni**$^+$-$B(C_6F_5)_4^-$ (46.0 mg, 33.6 μmol, 77%) as a purple solid. R_f = 0.70 (5% MeOH/CH_2Cl_2). The signals in ^{1}H NMR (600 MHz, $CDCl_3$, 20 °C), observed at 9.88 (s, 2H, β-CH), 9.00 (s, 4H, β-CH), 8.90 (s, 2H, β-CH), 8.15–8.13 (m, 4H, Ph-H), 8.07–8.05 (m, 4H, Ph-H), 7.91–7.85 (m, Ph-H), and 7.81–7.79 (m, 4H, Ph-H) ppm, were too broad to discuss in detail, whereas the signals in $^{13}C\{^1H\}$ NMR (151 MHz, $CDCl_3$, 20 °C) were not fully detected. UV/vis (CH_2Cl_2, λ_{max}[nm] (ε, 10^5 $M^{-1}cm^{-1}$)): 290 (0.22), 431 (1.1), 527 (0.10), 717 (0.026). HRMS (ESI-TOF) *m/z*: [M – $C_{24}BF_{20}$]$^+$ Calcd for $C_{44}H_{28}N_3SNi$ 688.1352; Found 688.1352. [M – $C_{44}H_{28}N_3SNi$]$^-$ Calcd for $C_{24}BF_{20}$ 678.9783; Found 678.9783. This compound was further characterized by single-crystal X-ray analysis.

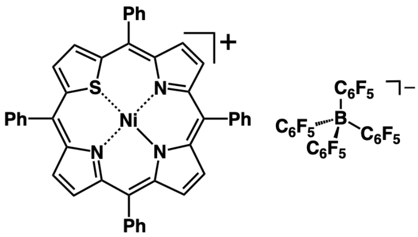

Ni^{II} complex of 5,10,15,20-tetraphenyl-21-thiaporphyrin as a PCCp$^-$ ion pair, 1ni$^+$-PCCp$^-$. To a MeOH solution (3 mL) of **1ni**$^+$-Cl$^-$ (9.49 mg, 13.1 μmol) was added sodium pentacyanocyclopentadienide (NaPCCp)[S3] (2.48 mg, 13.0 μmol) and the reaction mixture was stirred at r.t. for 1 h, followed by filtration and evaporation to dryness. The residue was purified by silica gel column chromatography (Wakogel C-300; eluent: 5% MeOH/CH_2Cl_2) and was recrystallized from CH_2Cl_2/*n*-hexane to afford **1ni**$^+$-PCCp$^-$ (7.05 mg, 8.01 μmol, 61%) as a purple solid. R_f = 0.68 (5% MeOH/CH_2Cl_2). ^{1}H NMR (600 MHz, $CDCl_3$, 20 °C): δ (ppm) 11.42 (s, 2H, β-CH), 10.13 (s, 2H, β-CH), 10.02 (s, 2H, β-CH), 8.45 (s, 2H, β-CH), 8.23 (d, J = 7.2 Hz, 4H, Ph-H), 8.16 (d, J = 6.6 Hz, 4H, Ph-H), 8.01 (t, J = 7.2 Hz, 4H, Ph-H), 7.90 (t, J = 7.2 Hz, 4H, Ph-H), 7.81 (t, J = 8.4 Hz, 4H, Ph-H) (the signals in ^{13}C{^{1}H} NMR (151 MHz, $CDCl_3$, 20 °C) were not fully detected). UV/vis (CH_2Cl_2, λ_{max}[nm] (ε, 10^5 $M^{-1}cm^{-1}$)): 292 (0.35), 431 (1.2), 526 (0.12), 715 (0.031). HRMS (ESI-TOF) *m/z*: [M – $C_{10}N_5$]$^+$ Calcd for $C_{44}H_{28}N_3SNi$ 688.1352; Found 688.1352. [M – $C_{44}H_{28}N_3SNi$]$^-$) Calcd for $C_{10}N_5$ 190.0157; Found 190.0157. This compound was further characterized by single-crystal X-ray analysis.

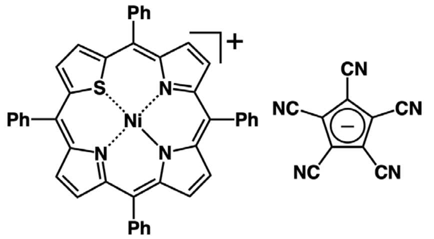

[S1] L. Latos-Grażyński, J. Lisowski, M. M. Olmstead and A. L. Balch, *Inorg. Chem.*, 1989, **28**, 1183–1188.

[S2] (a) C. E. Stilts, M. I. Nelen, D. G. Hilmey, S. R. Davies, S. O. Gollnick, A. R. Oseroff, S. L. Gibson, R. Hilf and M. R. Detty, *J. Med. Chem.*, 2000, **43**, 2403–2410; (b) D. G. Hilmey, M. Abe, M. I. Nelen, C. E. Stilts, G. A. Baker, S. N. Baker, F. V. Bright, S. R. Davies, S. O. Gollnick, A. R. Oseroff, S. L. Gibson, R. Hilf and M. R. Detty, *J. Med. Chem.*, 2002, **45**, 449–461.

[S3] (a) O. W. Webster, *J. Am. Chem. Soc.*, 1965, **87**, 1820–1821; (b) T. Sakai, S. Seo, J. Matsuoka and Y. Mori, *J. Org. Chem.*, 2013, **78**, 10978–10985.

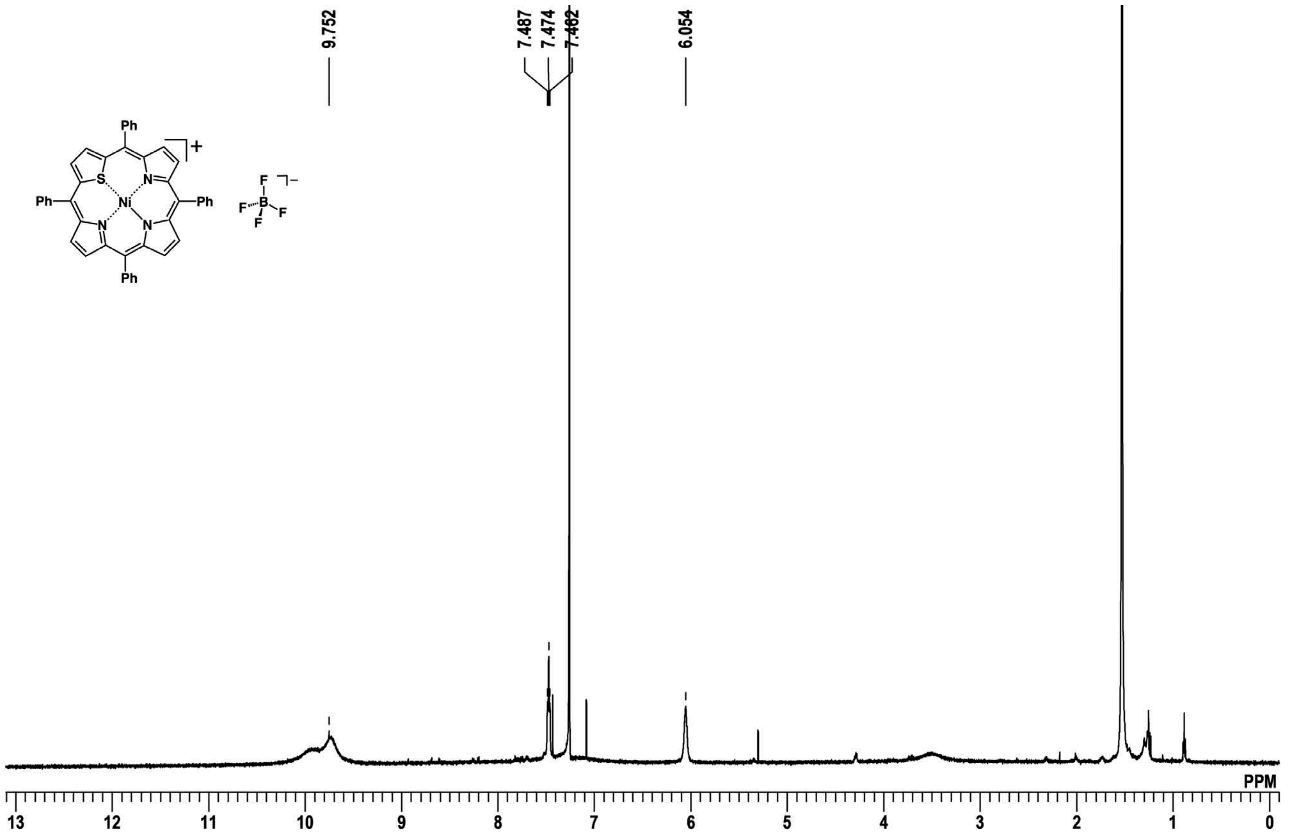

Fig. S1 ^{1}H NMR spectrum of **1ni**$^{+}$-BF_4^{-} in $CDCl_3$ at 20 °C.

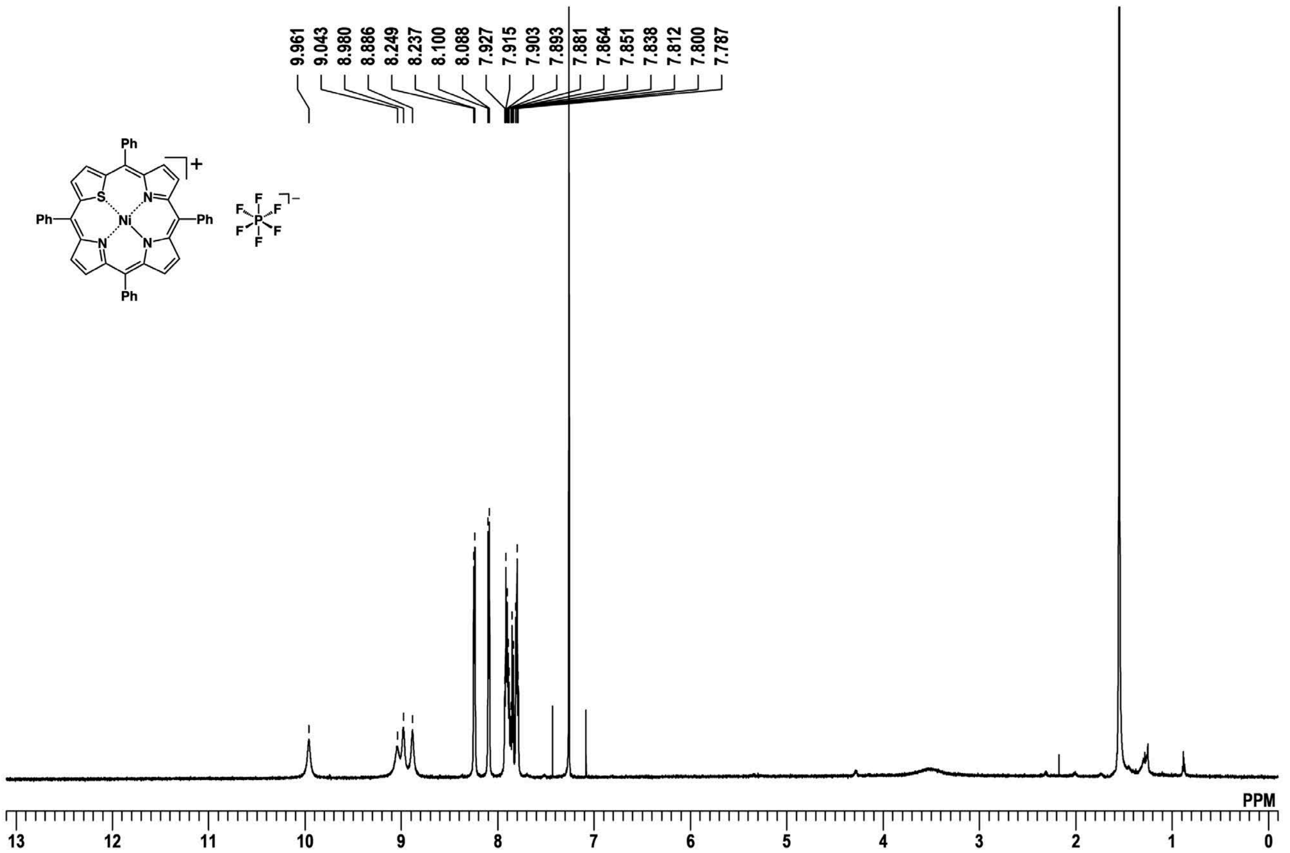

Fig. S2 ^{1}H NMR spectrum of **1ni**$^{+}$-PF_6^{-} in $CDCl_3$ at 20 °C.

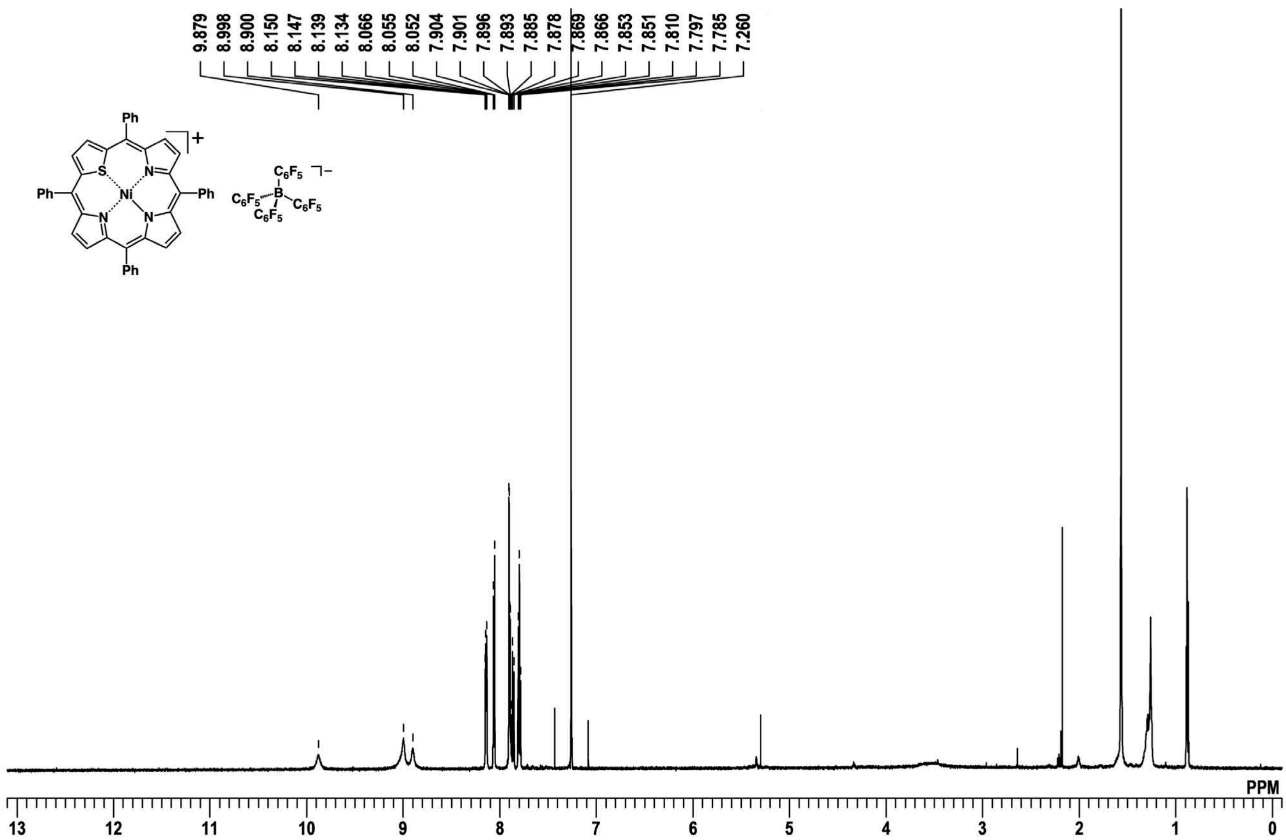

Fig. S3 ^{1}H NMR spectrum of **1ni**$^+$-$B(C_6F_5)_4^-$ in $CDCl_3$ at 20 °C.

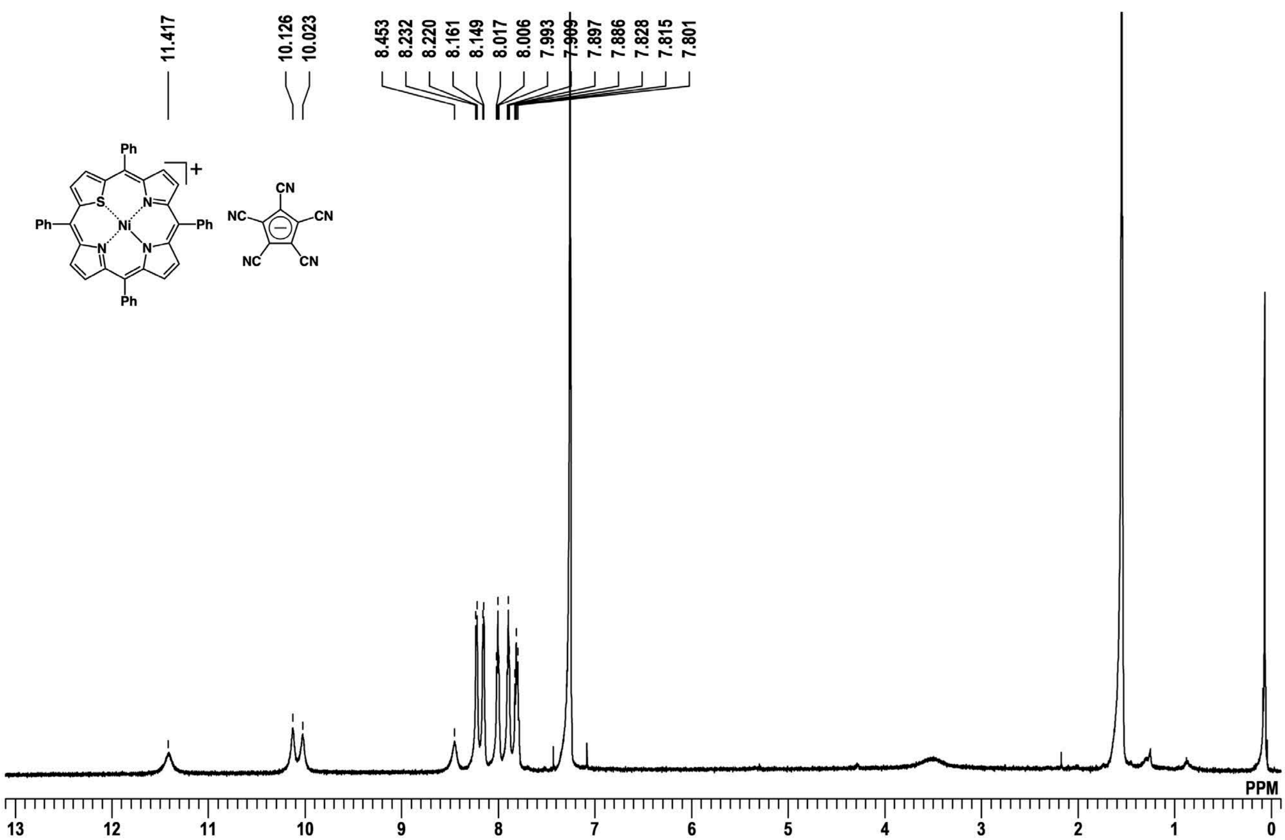

Fig. S4 ^{1}H NMR spectrum of **1ni**$^+$-PCCp$^-$ in $CDCl_3$ at 20 °C.

2. X-ray crystallographic data

Method for single-crystal X-ray analysis. Crystallographic data are summarized in Table S1. A single crystal of **1ni**$^{+}$-Cl$^{-}_{tri}$ was obtained by vapor diffusion of *n*-hexane into a $CHCl_3$ solution. The data crystal was a brown prism of approximate dimensions 0.30 mm × 0.20 mm × 0.20 mm. A single crystal of **1ni**$^{+}$-Cl$^{-}_{ortho}$ was obtained by vapor diffusion of *n*-pentane into a THF solution in the presence of 1,3-bis(3,4-diethylpyrrol-2-yl)-1,3-propanedione BF_2 complex[S4] **2b** (1 equiv). The data crystal was a purple plate of approximate dimensions 0.240 mm × 0.100 mm × 0.056 mm. A single crystal of **1ni**$^{+}$-PF_6^{-} was obtained by vapor diffusion of *n*-pentane into a CH_2Cl_2 solution. The data crystal was a brown prism of approximate dimensions 0.350 mm × 0.152 mm × 0.110 mm. A single crystal of **1ni**$^{+}$-$B(C_6F_5)_4^{-}$ was obtained by vapor diffusion of *n*-hexane into a chlorobenzene solution. The data crystal was a brown block of approximate dimensions 0.02 mm × 0.02 mm × 0.01 mm. A single crystal of **1ni**$^{+}$-PCCp^{-} was obtained by vapor diffusion of *n*-hexane into a CH_2Cl_2 solution. The data crystal was a brown plate of approximate dimensions 0.10 mm × 0.10 mm × 0.08 mm. A single crystal of **1ni**$^{+}$-**2a**·Cl^{-} was obtained by vapor diffusion of *n*-hexane into a CH_2Cl_2 solution of **1ni**$^{+}$-Cl^{-} and 1,3-di(pyrrol-2-yl)-1,3-propanedione BF_2 complex[S5] **2a** in the 1:1 ratio. The data crystal was a brown plate of approximate dimensions 0.30 mm × 0.30 mm × 0.10 mm. A single crystal of **1ni**$^{+}$-**2b**·Cl^{-} was obtained by vapor diffusion of *n*-hexane into a CCl_4 solution of **1ni**$^{+}$-Cl^{-} and **2b** in the 1:1 ratio. The data crystal was a brown block of approximate dimensions 0.100 mm × 0.050 mm × 0.030 mm. A single crystal of **1ni**$^{+}$-**2c**·Cl^{-} was obtained by vapor diffusion of *n*-hexane into a $CHCl_3$ solution of **1ni**$^{+}$-Cl^{-} and 1,3-bis(3,4-difluoropyrrol-2-yl)-1,3-propanedione BF_2 complex[S6] **2c** in the 1:1 ratio. The data crystal was a purple block of approximate dimensions 0.05 mm × 0.03 mm × 0.03 mm. The data of **1ni**$^{+}$-Cl$^{-}_{tri}$, **1ni**$^{+}$-PCCp^{-}, and **1ni**$^{+}$-**2a**·Cl^{-} were collected at 90 K on a Bruker D8 Venture diffractometer with MoKα radiation (λ = 0.71073 Å) focused by multilayer confocal mirror, whereas those of **1ni**$^{+}$-Cl$^{-}_{ortho}$, **1ni**$^{+}$-PF_6^{-}, and **1ni**$^{+}$-**2b**·Cl^{-} were collected at 100 K on a DECTRIS PILATUS3 CdTe 1M diffractometer with Si (311) monochromated synchrotron radiation (λ = 0.4125, 0.4125, and 0.4127 Å, respectively) at BL02B1 (SPring-8).[S7] The data of **1ni**$^{+}$-$B(C_6F_5)_4^{-}$ and **1ni**$^{+}$-**2c**·Cl^{-} were collected at 90 K on a Dectris EIGER X 1M diffractometer with Si (111) monochromated synchrotron radiation (λ = 0.81106 and 0.81063 Å, respectively) at BL40XU (SPring-8).[S8] All the structures were solved by dual-space method. The structures were refined by a full-matrix least-squares method by using a SHELXL 2014[S9] (Yadokari-XG).[S10] In each structure, the non-hydrogen atoms were refined anisotropically. CIF files (CCDC-2167300–2167307) can be obtained free of charge from the Cambridge Crystallographic Data Centre via www.ccdc.cam.ac.uk/data_request/cif.

Table S1 Crystallographic details.

	1ni$^+$-Cl^-_{tri}	**1ni**$^+$-Cl^-_{ortho}	**1ni**$^+$-PF_6^-	**1ni**$^+$-$B(C_6F_5)_4^-$	**1ni**$^+$-$PCCp^-$
formula	$C_{44}H_{28}N_3SClNi\cdot C_6H_{14}\cdot CHCl_3$	$C_{44}H_{28}N_3SClNi\cdot C_4H_8O$	$C_{44}H_{28}N_3SNi\cdot PF_6\cdot 2CH_2Cl_2$	$C_{44}H_{28}N_3SNi\cdot C_{24}BF_{20}\cdot C_6H_5Cl$	$C_{44}H_{28}N_3SNi\cdot C_{10}N_5\cdot 2CH_2Cl_2$
fw	930.45	797.02	1004.28	1481.06	1049.46
crystal size, mm	0.30 × 0.20 × 0.20	0.240 × 0.100 × 0.056	0.350 × 0.152 × 0.110	0.02× 0.02 × 0.01	0.10 × 0.10 × 0.08
crystal system	triclinic	orthorhombic	monoclinic	triclinic	triclinic
space group	$P\bar{1}$ (no. 2)	*Pbca* (no. 61)	$P2_1/c$ (no. 14)	$P\bar{1}$ (no. 2)	$P\bar{1}$ (no. 2)
a, Å	11.8089(9)	14.864(3)	13.771(3)	13.2112(3)	13.9345(12)
b, Å	12.2573(10)	23.185(4)	16.0517(19)	15.9096(4)	15.3744(14)
c, Å	17.3475(15)	21.949(4)	19.023(3)	16.7024(4)	24.075(2)
α, °	80.827(3)	90	90	62.936(2)	79.220(4)
β, °	78.140(3)	90	90.485(6)	87.227(2)	89.861(3)
γ, °	66.538(3)	90	90	74.503(2)	69.239(4)
V, Å^3	2245.8(3)	7564(2)	4204.8(12)	3001.55(14)	4726.2(7)
ρ_{calcd}, gcm^{-3}	1.376	1.400	1.586	1.639	1.475
Z	2	8	4	2	4
T, K	90(2)	100(2)	100(2)	90(2)	90(2)
μ, mm^{-1}	0.756 ^{a}	0.164 ^{b}	0.202 ^{b}	0.732 ^{b}	0.731 ^{a}
no. of reflns	35077	215930	123301	31511	77297
no. of unique reflns	15737	8587	9657	10942	32350
variables	553	533	661	883	1345
λ, Å	0.71073 ^{a}	0.4125 ^{b}	0.4125 ^{b}	0.81106 ^{b}	0.71073 ^{a}
R_1 ($I > 2\sigma(I)$)	0.1028	0.0391	0.0764	0.0673	0.0811
wR_2 ($I > 2\sigma(I)$)	0.2512	0.0938	0.1800	0.1463	0.1775
GOF	1.043	1.085	1.060	1.066	1.049

	1ni$^+$-**2a**$\cdot Cl^-$	**1ni**$^+$-**2b**$\cdot Cl^-$	**1ni**$^+$-**2c**$\cdot Cl^-$
formula	$C_{44}H_{28}N_3SClNi\cdot C_{11}H_9BN_2O_2F_2\cdot 1.258CH_2Cl_2$	$C_{44}H_{28}N_3SClNi\cdot C_{19}H_{25}BN_2O_2F_2\cdot 2CCl_4$	$C_{44}H_{28}N_3SClNi\cdot C_{11}H_5BN_2O_2F_6\cdot H_2O$
fw	1083.45	1394.75	1064.91
crystal size, mm	0.30 × 0.30 × 0.10	0.100 × 0.050 × 0.030	0.05 × 0.03 × 0.03
crystal system	triclinic	monoclinic	triclinic
space group	$P\bar{1}$ (no. 2)	$P2_1/c$ (no.14)	$P\bar{1}$ (no. 2)
a, Å	13.066(3)	12.962(9)	12.3536(4)
b, Å	13.295(3)	17.107(12)	13.2407(4)
c, Å	15.987(4)	27.519(15)	14.7731(5)
α, °	113.935(9)	90	83.126(3)
β, °	91.484(8)	102.088(18)	84.024(3)
γ, °	92.340(8)	90	81.561(3)
V, Å^3	2533.5(10)	5967(7)	2363.86(13)
ρ_{calcd}, gcm^{-3}	1.420	1.553	1.496
Z	2	4	2
T, K	90(2)	100(2)	90(2)
μ, mm^{-1}	0.668 ^{a}	0.190 ^{b}	0.834 ^{b}
no. of reflns	37396	131879	18843
no. of unique reflns	17602	10531	8458
variables	677	816	692
λ, Å	0.71073 ^{a}	0.4127 ^{b}	0.81063 ^{b}
R_1 ($I > 2\sigma(I)$)	0.0963	0.1067	0.0519
wR_2 ($I > 2\sigma(I)$)	0.2626	0.3905	0.1183
GOF	1.016	1.997	1.127

^{a} The values under the Mo-Kα radiation. ^{b} The values under the synchrotron radiation.

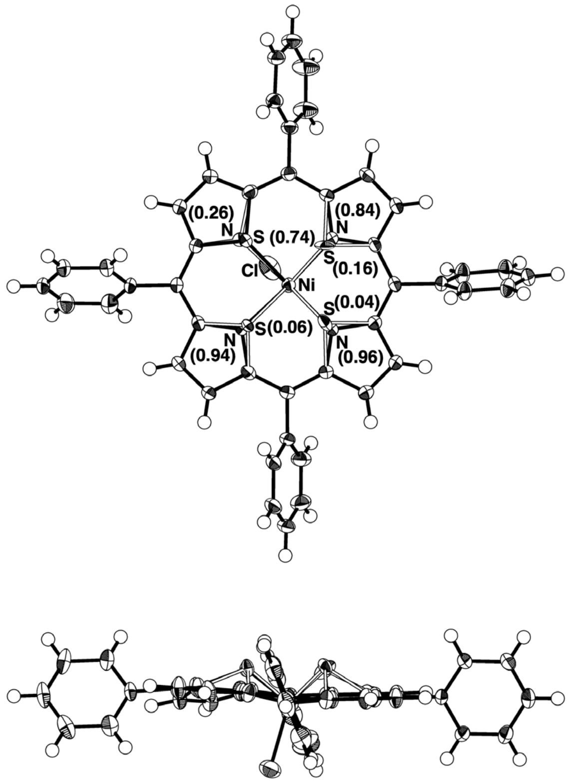

Fig. S5 Ortep drawing of single-crystal X-ray structure (top and side views) of **1ni**$^{+}$-Cl$^{-}_{\mathrm{tri}}$ as a pseudopolymorph of **1ni**$^{+}$-Cl^{-} in the previous study.[S1] Disordered structures are represented by black and white bonds for major and minor structures, respectively, in the ratio of 74 : 16 : 6 : 4 for the porphyrin inner atoms (according to the existence of sulfur). Thermal ellipsoids are scaled to the 50% probability level. Solvent molecules are omitted for clarity.

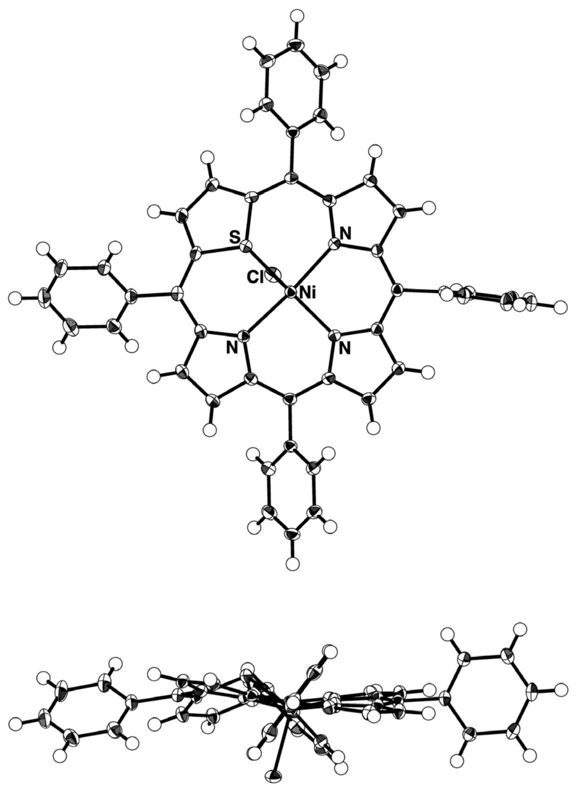

Fig. S6 Ortep drawing of single-crystal X-ray structure (top and side views) of **1ni**$^{+}$-Cl$^{-}_{\mathrm{ortho}}$ as a pseudopolymorph of **1ni**$^{+}$-Cl^{-} in the previous study.[S1] Thermal ellipsoids are scaled to the 50% probability level. Solvent molecules are omitted for clarity.

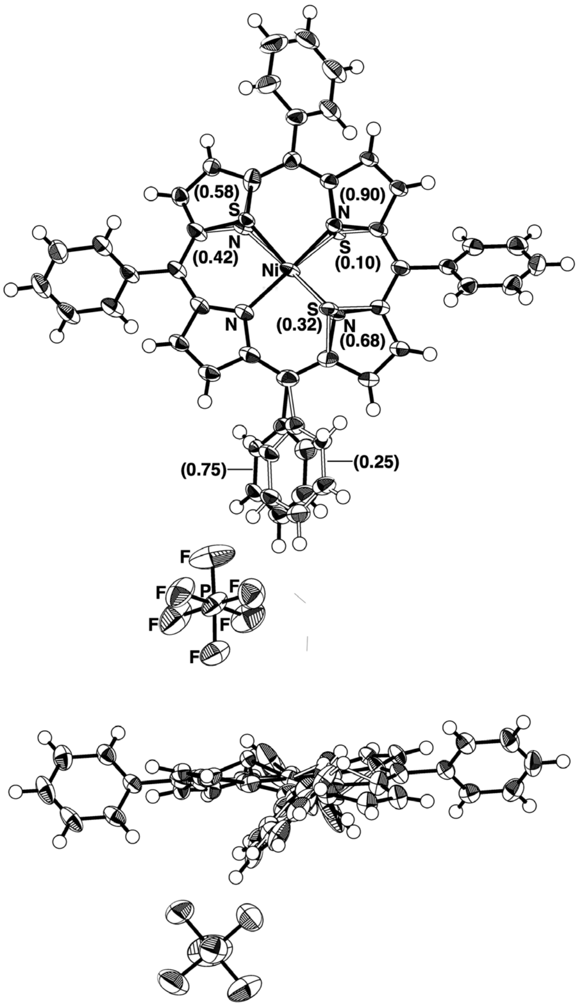

Fig. S7 Ortep drawing of single-crystal X-ray structure (top and side view) of **1ni**$^{+}$-PF_6^{-}. Disordered structures are represented by black and white bonds for major and minor structures, respectively, in the ratios of 58 : 32 : 10 and 75 : 25 for the porphyrin inner atoms (according to the existence of sulfur) and a phenyl group, respectively. Thermal ellipsoids are scaled to the 50% probability level. Solvent molecules are omitted for clarity.

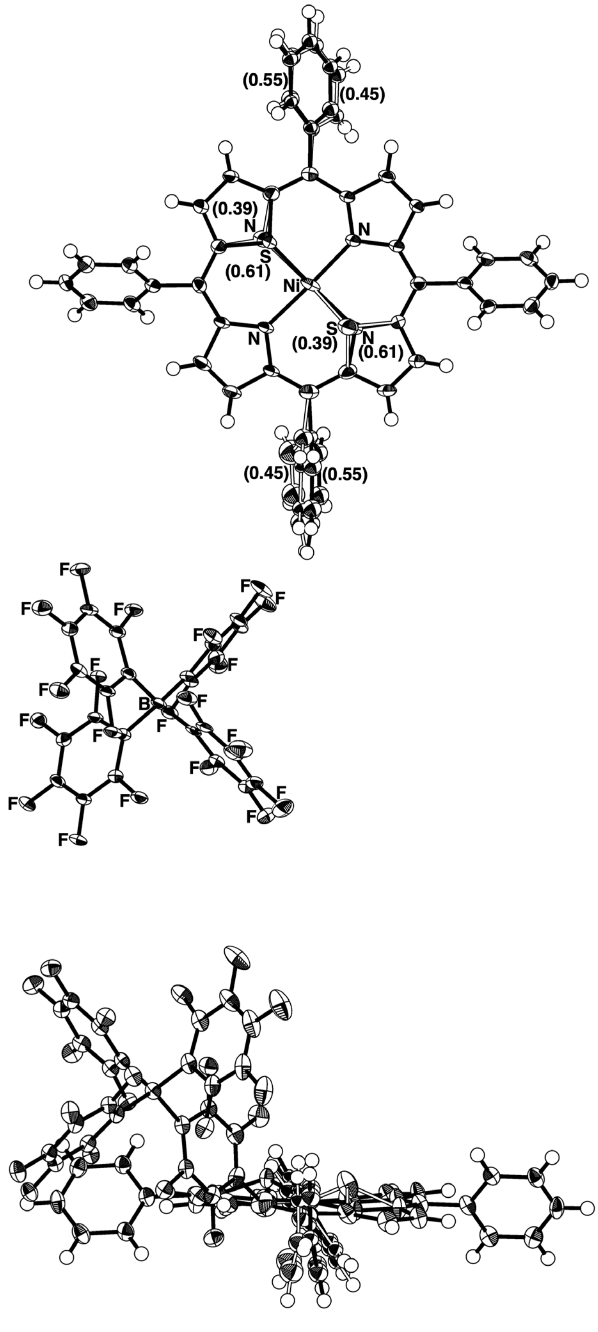

Fig. S8 Ortep drawing of single-crystal X-ray structure (top and side view) of **1ni**$^+$-B(C_6F_5)$_4^-$. Disordered structures are represented by black and white bonds for major and minor structures, respectively, in the ratios of 61 : 39 and 55 : 45 for the porphyrin inner atoms (according to the existence of sulfur) and a phenyl group, respectively. Thermal ellipsoids are scaled to the 50% probability level. Solvent molecules are omitted for clarity.

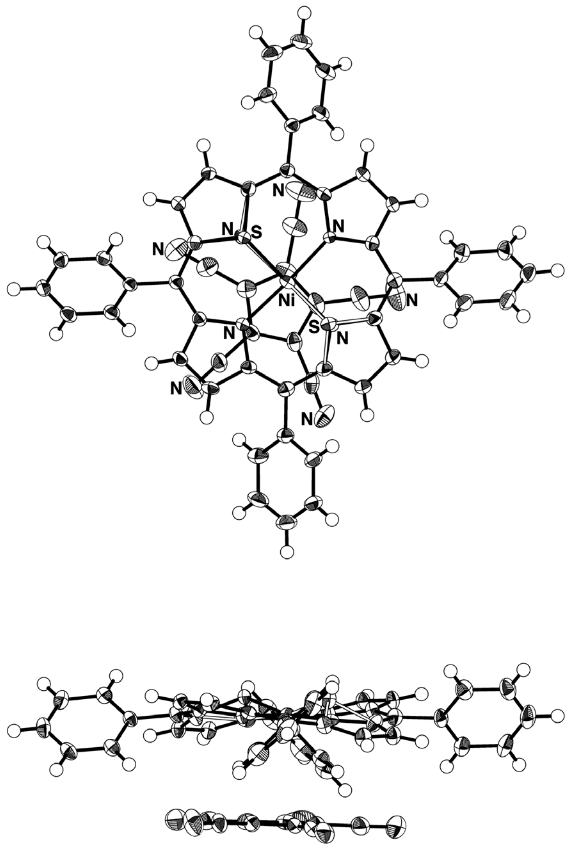

Fig. S9 Ortep drawing of single-crystal X-ray structure (top and side views) of **1ni**$^{+}$-PCCp^{-}. Disordered structures are represented by black and white bonds for major and minor structures, respectively, in the ratio of 72 : 28 for the porphyrin inner atoms (according to the existence of sulfur). Thermal ellipsoids are scaled to the 50% probability level. Solvent molecules are omitted for clarity.

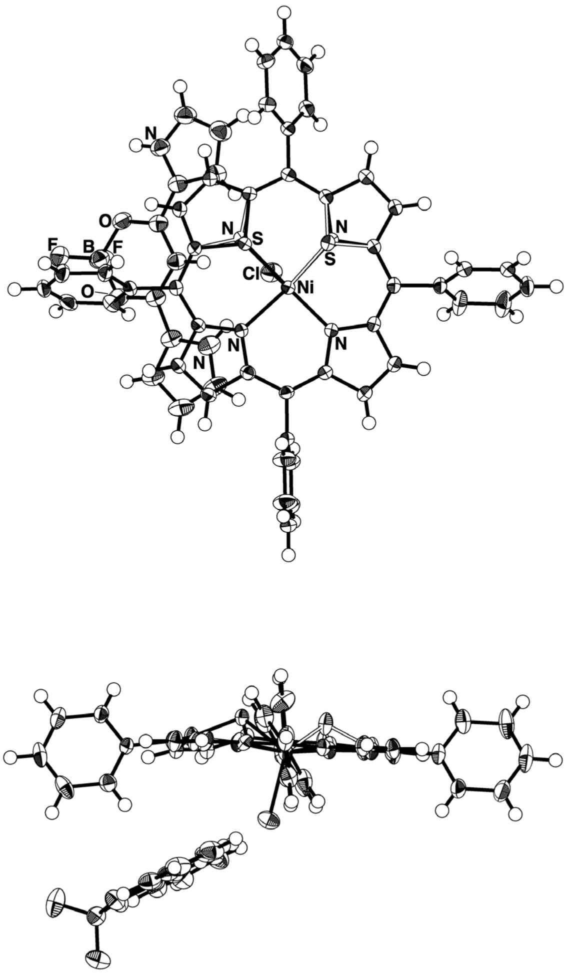

Fig. S10 Ortep drawing of single-crystal X-ray structure (top and side views) of **1ni**$^{+}$-**2a**·Cl^{-}. Disordered structures are represented by black and white bonds for major and minor structures, respectively, in the ratio of 88 : 12 for the porphyrin inner atoms (according to the existence of sulfur). Thermal ellipsoids are scaled to the 50% probability level. Solvent molecules are omitted for clarity.

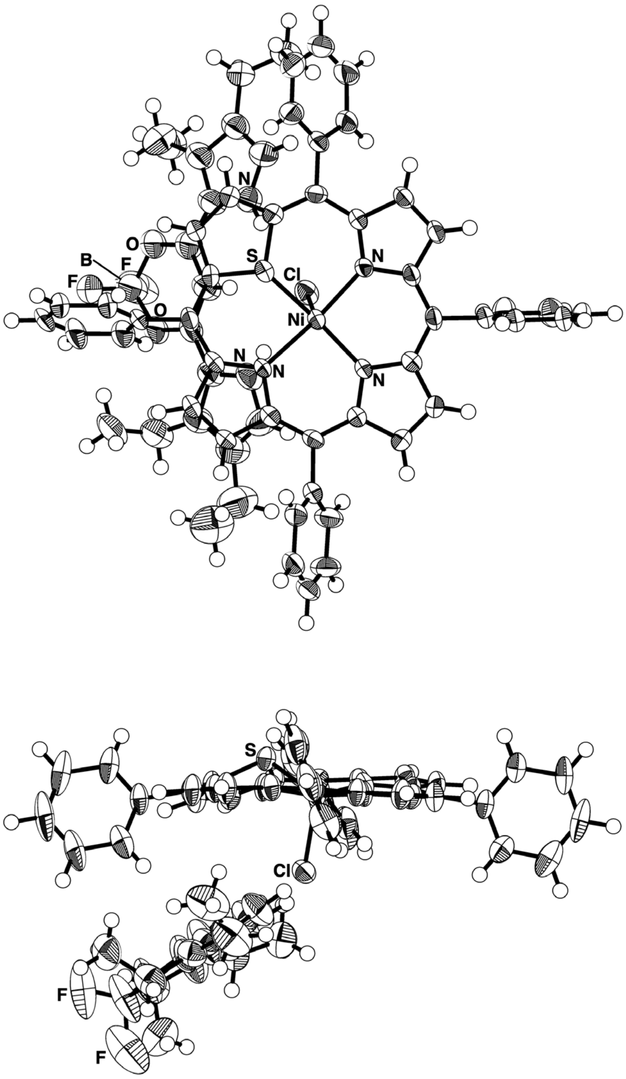

Fig. S11 Ortep drawing of single-crystal X-ray structure (top and side views) of **1ni**$^{+}$-**2b**·Cl^{-}. Thermal ellipsoids are scaled to the 50% probability level. Solvent molecules are omitted for clarity.

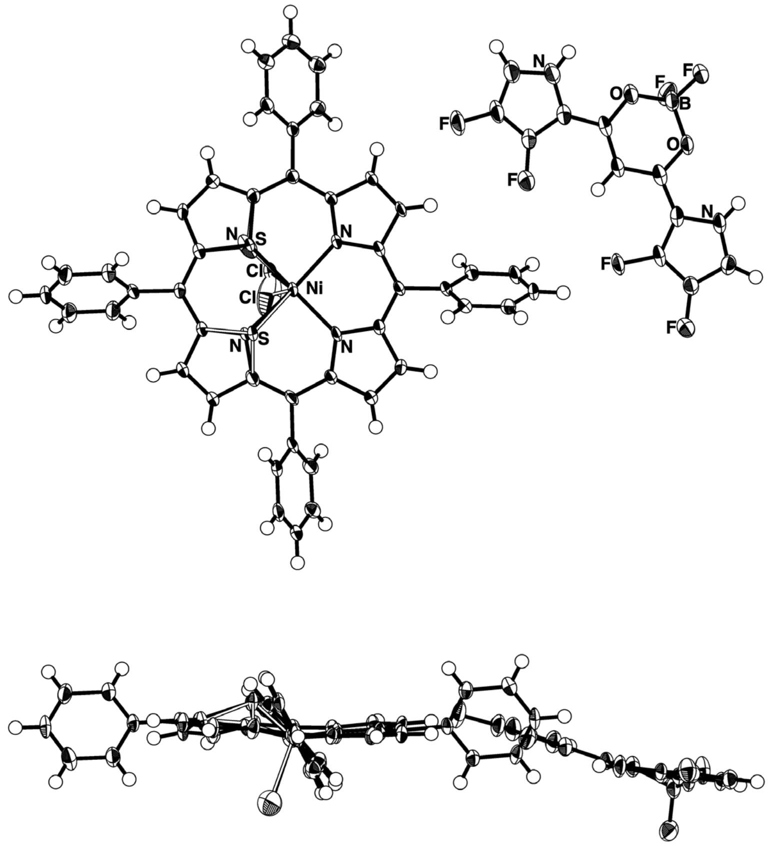

Fig. S12 Ortep drawing of single-crystal X-ray structure (top and side views) of **1ni**$^{+}$-**2c**·Cl^{-}. Disordered structures are represented by black and white bonds for major and minor structures, respectively, in the ratio of 80 : 20 for the porphyrin inner atoms (according to the existence of sulfur) and chlorine, respectively. Thermal ellipsoids are scaled to the 50% probability level. Solvent molecules are omitted for clarity.

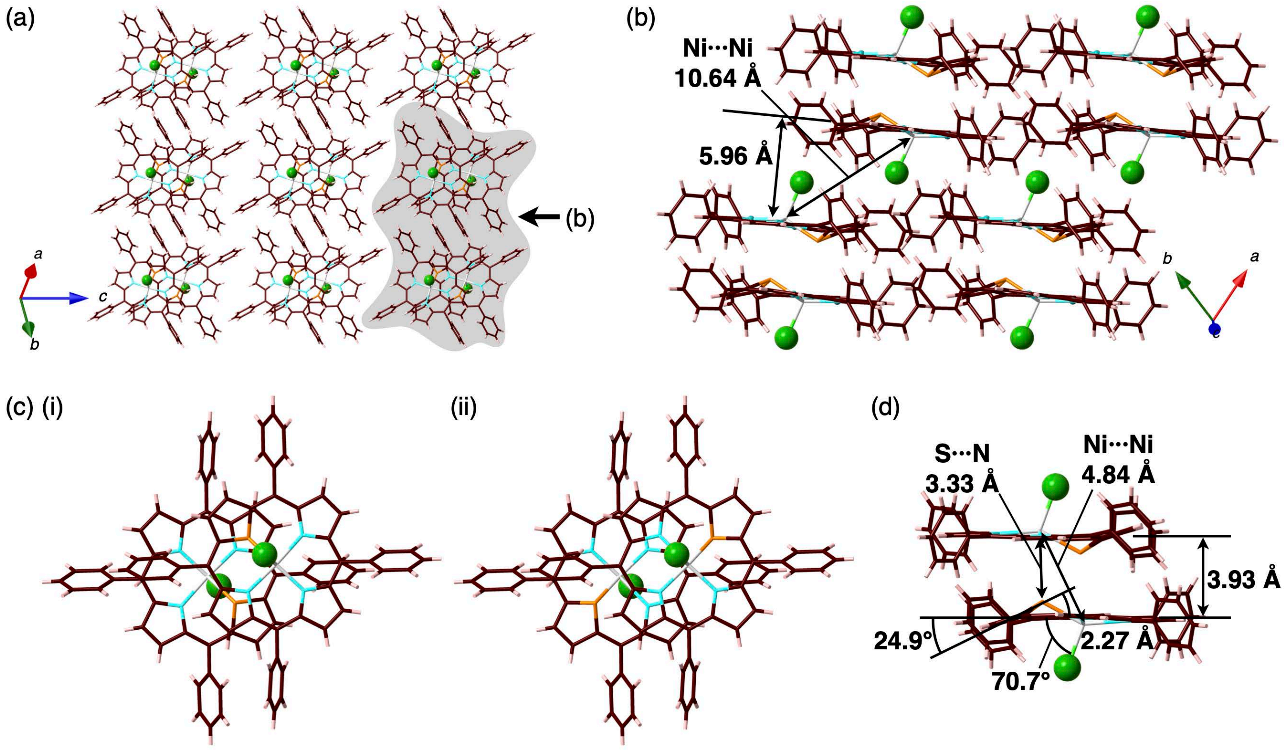

Fig. S13 Packing diagram (stacking assembly) of **1ni**$^{+}$-Cl$^{-}_{tri}$ as (a) a top view and (b) a side view from the arrow shown in (a), (c) top views of the dimers as (i) major (74%) and (ii) second major (16%) structures (Fig. S5), and (d) side view of the major dimer. The stacking distances between two **1ni**$^{+}$ (core 25 atoms) and the Ni···Ni distances in the column are 3.93/5.96 and 4.84/10.64 Å, respectively. The Ni–Cl distance is 2.27 Å and the angle of the line through Ni and Cl^{-} to the core porphyrin plane (25 atoms) is 70.7°. The S···N distance in two stacking **1ni**$^{+}$ units is 3.33 Å and the dihedral angle between the thiophene plane and the core porphyrin plane (25 atoms) is 24.9°. Mean-plane deviation of the **1ni**$^{+}$ core part (25 atoms) and τ_4 value[S11] are 0.20 Å and 0.36, respectively. Atom color code: brown, pink, blue, orange, green, and light gray refer to carbon, hydrogen, nitrogen, sulfur, chlorine, and nickel, respectively. Solvent molecules are omitted for clarity.

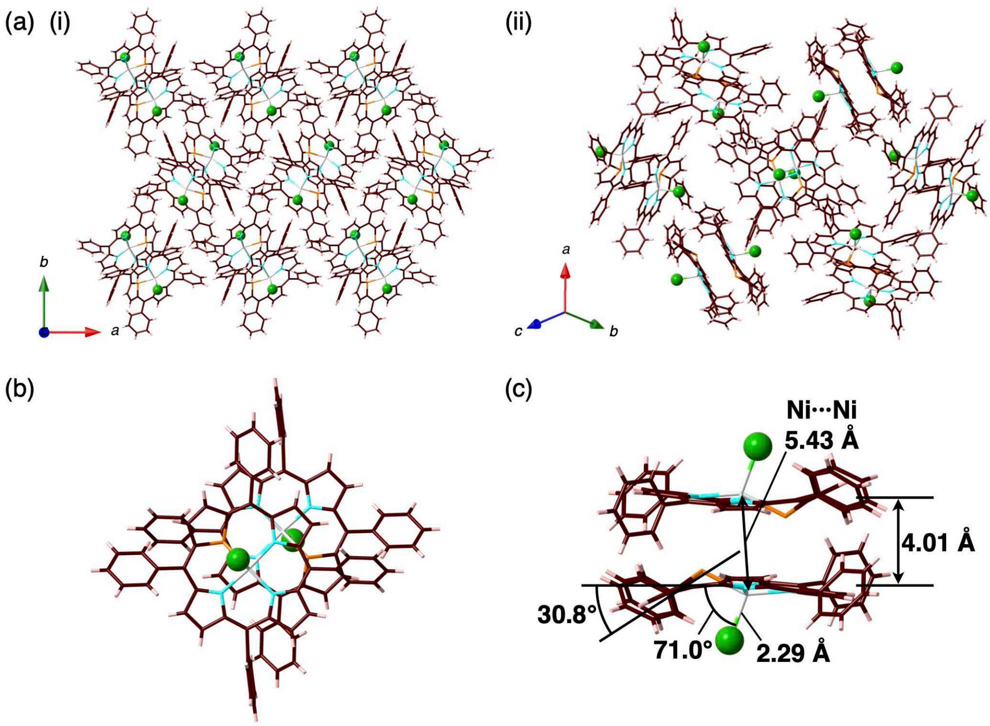

Fig. S14 (a) Packing diagram (stacking assembly) of **1ni**$^+$-Cl$^-_{ortho}$ as (i) a view along *c* axis and (ii) another view, (b) top view of the dimer, and (c) side view of the dimer. The stacking distances between two **1ni**$^+$ (core 25 atoms) and the Ni···Ni distances are 4.01 and 5.43 Å, respectively. The Ni–Cl distance is 2.29 Å and the dihedral angle of the line through Ni and Cl$^-$ to the core porphyrin plane (25 atoms) is 71.0°. The dihedral angle between the thiophene plane and the core porphyrin plane (25 atoms) is 30.8°. Mean-plane deviation of the **1ni**$^+$ core part (25 atoms) and τ_4 value[S11] are 0.30 Å and 0.36, respectively. Atom color code: brown, pink, blue, orange, green, and light gray refer to carbon, hydrogen, nitrogen, sulfur, chlorine, and nickel, respectively. Solvent molecules are omitted for clarity.

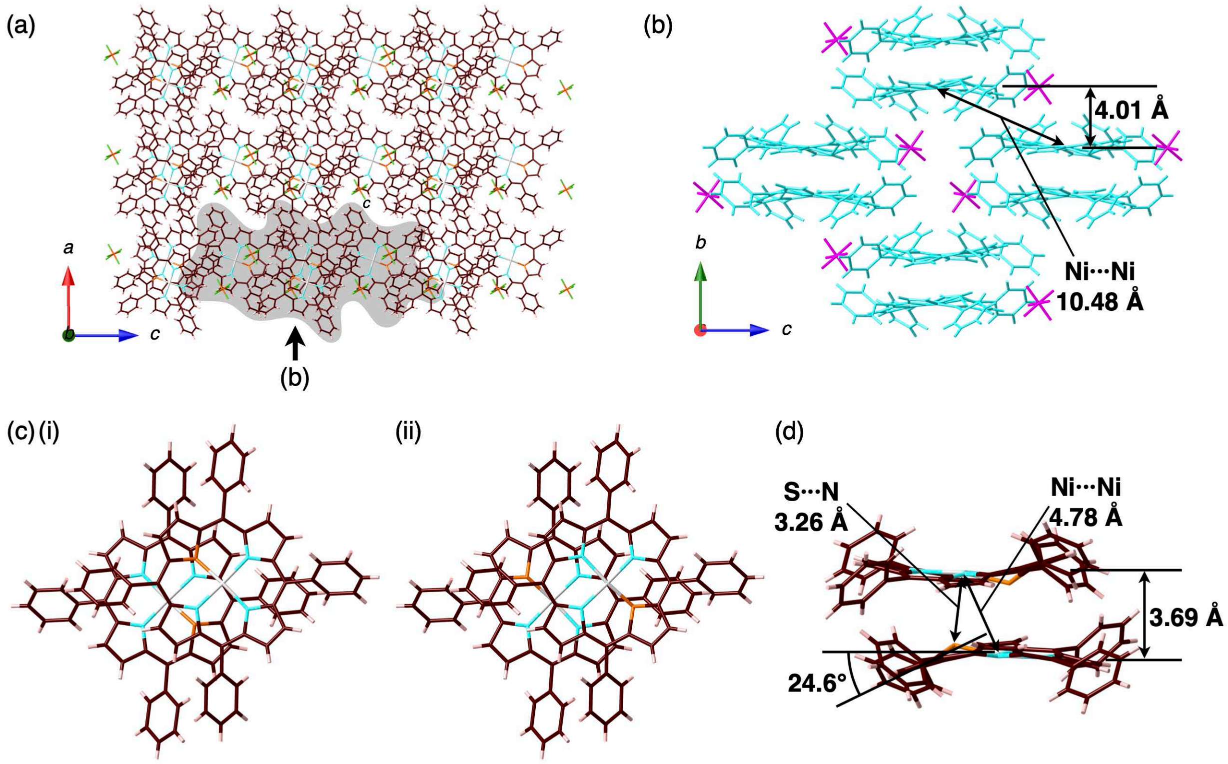

Fig. S15 Packing diagram (stacking assembly) of **1ni**$^+$-PF_6^- as (a) a top view and (b) a side view from the arrow shown in (a), (c) top views of the dimers as (i) major (58%) and (ii) second major (32%) structures (Fig. S7), and (d) side view of the dimer. The stacking distances between two **1ni**$^+$ (core 25 atoms) and the Ni···Ni distances in the column are 3.69/4.01 and 4.78/10.48 Å, respectively. The S···N distance in two stacking **1ni**$^+$ units is 3.26 Å and the dihedral angle between the thiophene plane and the core porphyrin plane (25 atoms) is 24.6°. Mean-plane deviation of the **1ni**$^+$ core part (25 atoms) and τ_4 value[S11] are 0.30 Å and 0.10, respectively. Atom color code: brown, pink, yellow green, blue, light orange, orange, and light gray refer to carbon, hydrogen, fluorine, nitrogen, phosphorus, sulfur, and nickel, respectively. Solvent molecules are omitted for clarity.

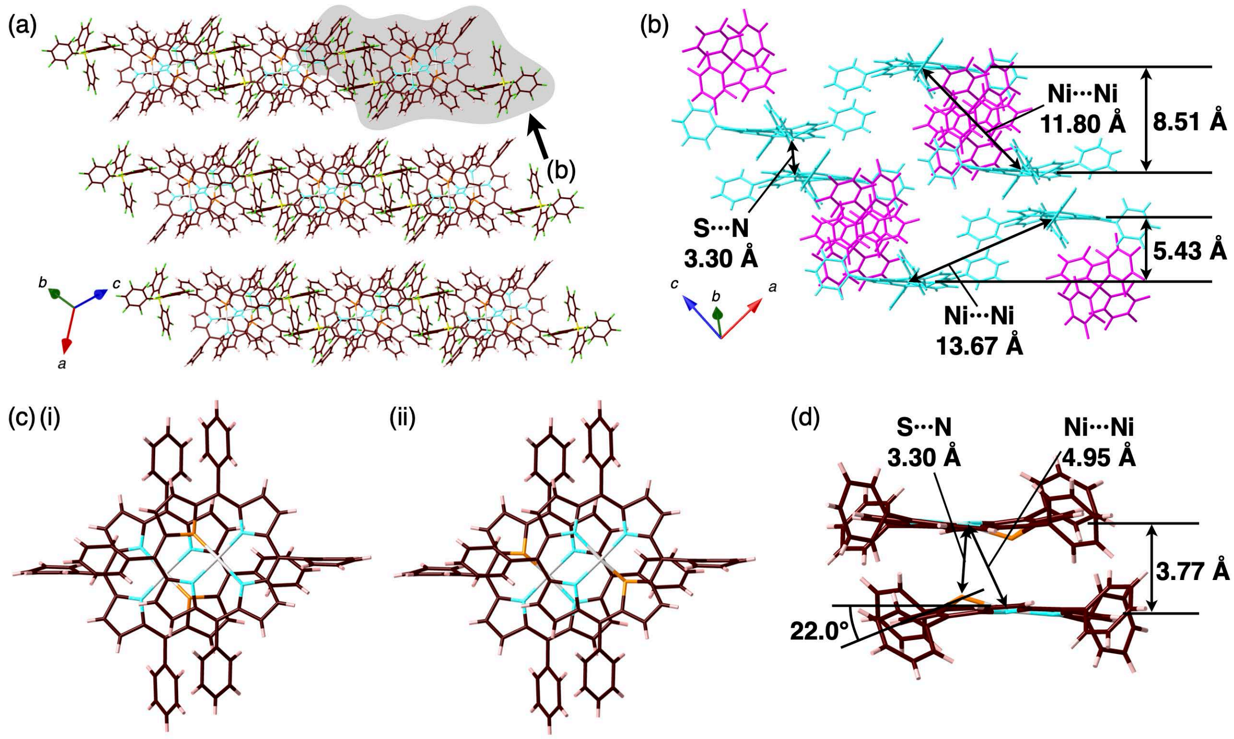

Fig. S16 (a) Packing diagram (stacking assembly) of **1ni**$^+$-B(C_6F_5)$_4^-$ as (a) a top view and (b) a side view, (c) top views of the dimers as (i) major (61%) and (ii) minor (39%) structures (Fig. S8), and (d) side view of the dimer. The distances between two **1ni**$^+$ (core 25 atoms) and the Ni···Ni distances are 3.77/5.43/8.51 and 4.95/13.67/11.80 Å, respectively. The S···N distance in two **1ni**$^+$ units in the column is 3.30 Å and the dihedral angle between the thiophene plane and the core porphyrin plane (core 25 atoms) is 22.0°. Mean-plane deviation of the **1ni**$^+$ core part (25 atoms) and τ_4 value[S11] are 0.21 Å and 0.10, respectively. Atom color code: brown, pink, yellow, blue, yellow green, orange, and light gray refer to carbon, hydrogen, boron, nitrogen, fluorine, sulfur, and nickel, respectively. Solvent molecules are omitted for clarity.

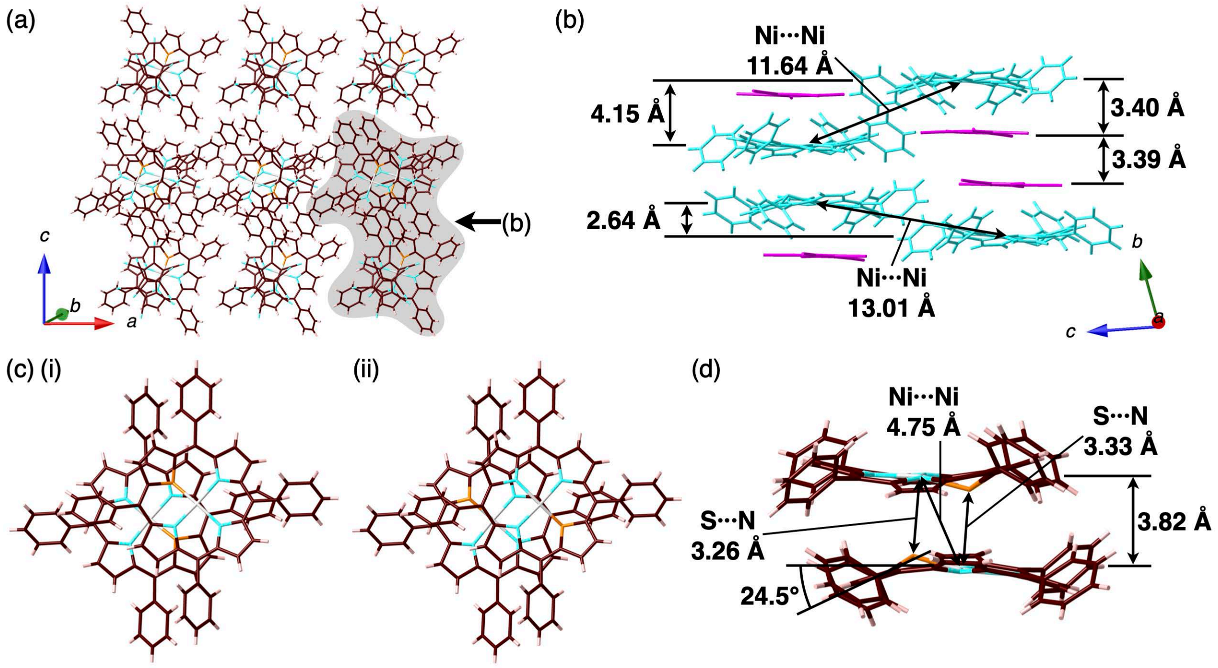

Fig. S17 Packing diagram (stacking assembly) of **1ni**$^{+}$-PCCp^{-} as (a) a top view and (b) a side view from the arrow shown in (a), (c) top views of the dimers as (i) major (72%) and (ii) minor (28%) structures (Fig. S9), and (d) side view of the dimer. The distances between two **1ni**$^{+}$, that between **1ni**$^{+}$ and PCCp^{-}, that between two PCCp^{-} (core 25 atoms), and the Ni···Ni distances in the column are 3.82/2.64/4.15, 3.40, 3.39, and 4.75/13.01/11.64 Å, respectively. The S···N distances in two stacking **1ni**$^{+}$ units are 3.26 and 3.33 Å and the dihedral angle between the thiophene plane and the core porphyrin plane (core 25 atoms) is 24.5°. Mean-plane deviation of the **1ni**$^{+}$ core part (25 atoms) and τ_4 value[S11] are 0.30 Å and 0.11, respectively. Atom color code: brown, pink, blue, orange, and light gray refer to carbon, hydrogen, nitrogen, sulfur, and nickel, respectively. Solvent molecules are omitted for clarity.

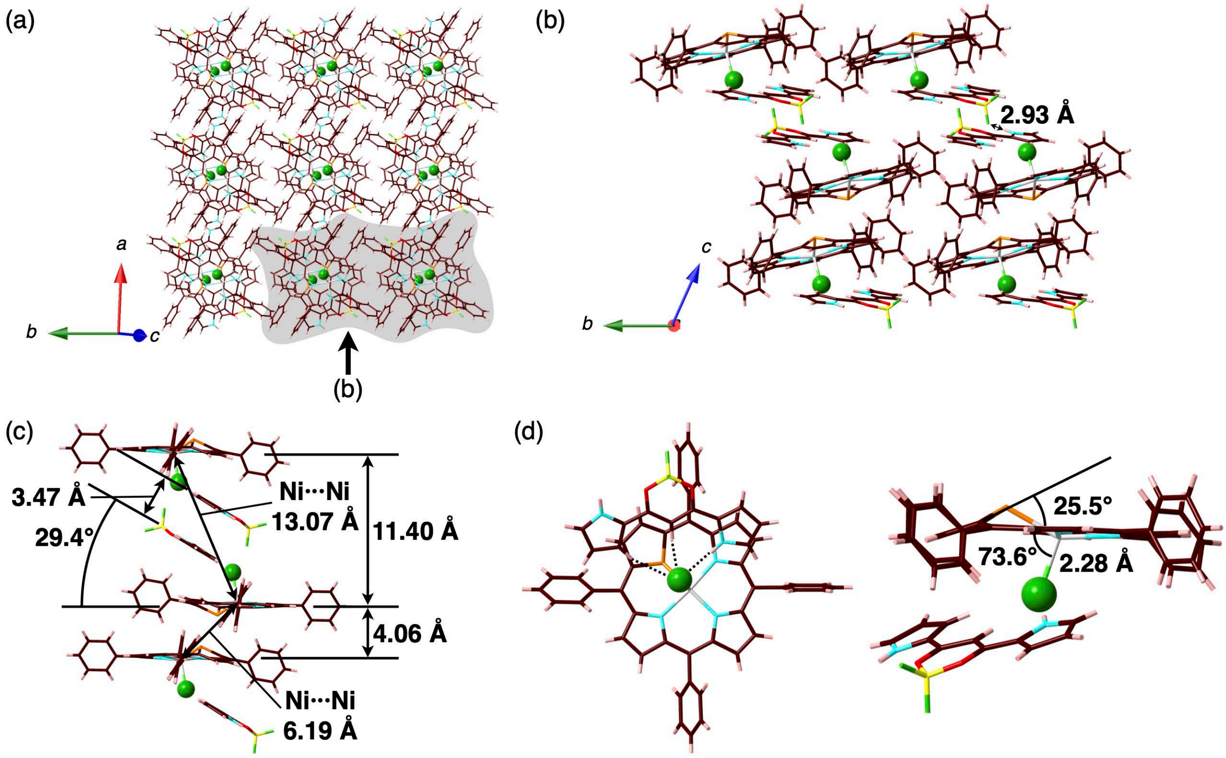

Fig. S18 Packing diagram (stacking assembly) of **1ni**$^{+}$-**2a**·Cl^{-} as (a) a top view and (b) a side view from the arrow shown in (a), (c) enlarged view of the packing structure, and (d) top and side views of the enlarged pair. The distances between two **1ni**$^{+}$-Cl^{-} (core 25 atoms), that between two **2a**, and the Ni···Ni distances in the column are 4.06/11.40, 3.47, and 6.19/13.07 Å, respectively. Pyrrole NH of **2a** interacts with the F unit of another **2a** with an N(–H)···F distance of 2.93 Å. Pyrrole NH, bridging CH, and pyrrole-β-CH interact with Cl^{-} with the N/C(–H)···Cl^{-} distances of 3.26, 3.52, and 3.79 Å, respectively. The Ni–Cl^{-} distance is 2.28 Å and the dihedral angle between the line through Ni and Cl^{-} to the core porphyrin plane (25 atoms) is 73.6°. The dihedral angle between the thiophene plane and the core porphyrin plane (core 25 atoms) is 25.5°. Mean-plane deviation of the **1ni**$^{+}$ core part (25 atoms) and τ_4 value[S11] are 0.20 Å and 0.33, respectively. Atom color code: brown, pink, yellow, blue, red, yellow green, orange, green, and light gray refer to carbon, hydrogen, boron, nitrogen, oxygen, fluorine, sulfur, chlorine, and nickel, respectively. Solvent molecules are omitted for clarity.

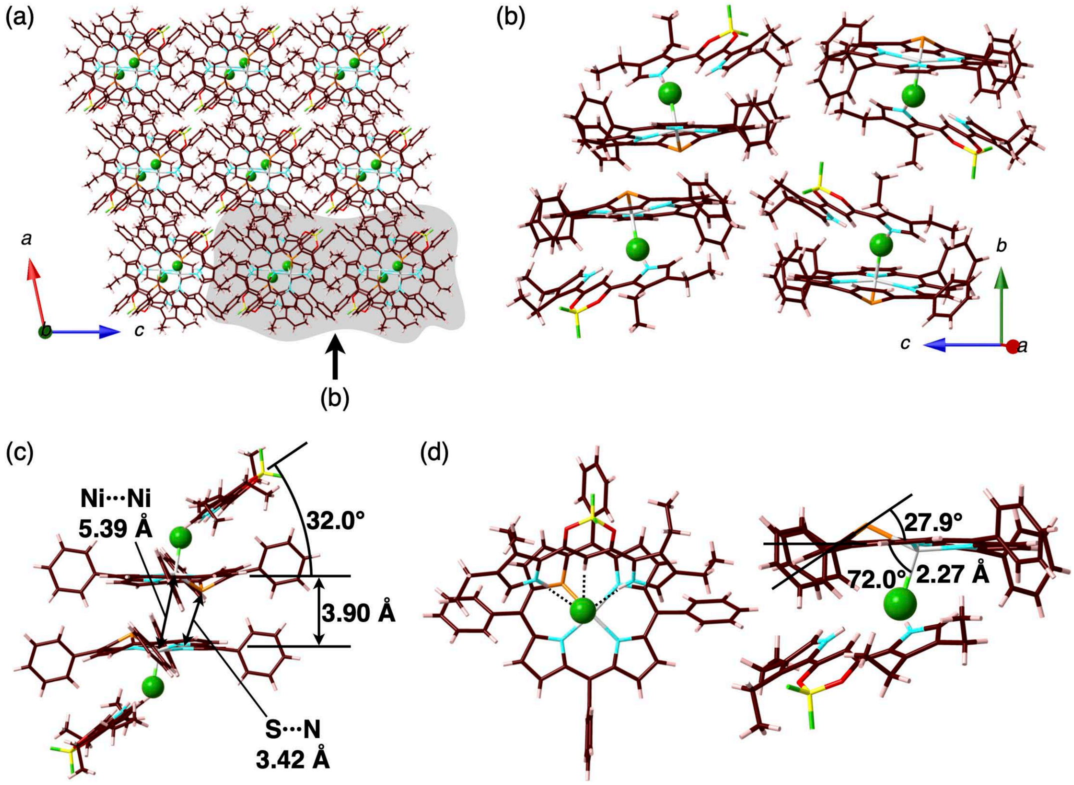

Fig. S19 Packing diagram (stacking assembly) of **1ni**$^+$-**2b**·Cl$^-$ as (a) a top view and (b) a side view from the arrow shown in (a), (c) enlarged view of the packing structure, and (d) top and side views of the enlarged pair. The stacking distance between two **1ni**$^+$-Cl$^-$ (core 25 atoms) and the Ni···Ni distance in the column are 3.90 and 5.39 Å, respectively. Two pyrrole NH and bridging CH interact with Cl$^-$ with the N/C(–H)···Cl$^-$ distances of 3.16/3.37 and 3.44 Å, respectively. The Ni–Cl$^-$ distance is 2.27 Å and the angle of the line through Ni and Cl$^-$ to the core porphyrin plane (25 atoms) is 72.0°. The S···N distance in two stacking **1ni**$^+$-Cl$^-$ units is 3.42 Å and the dihedral angle between the thiophene plane and the core porphyrin plane (core 25 atoms) is 27.9°. Mean-plane deviation of the **1ni**$^+$ core part (25 atoms) and τ_4 value[S11] are 0.22 Å and 0.33, respectively. Atom color code: brown, pink, yellow, blue, red, yellow green, orange, green, and light gray refer to carbon, hydrogen, boron, nitrogen, oxygen, fluorine, sulfur, chlorine, and nickel, respectively. Solvent molecules are omitted for clarity.

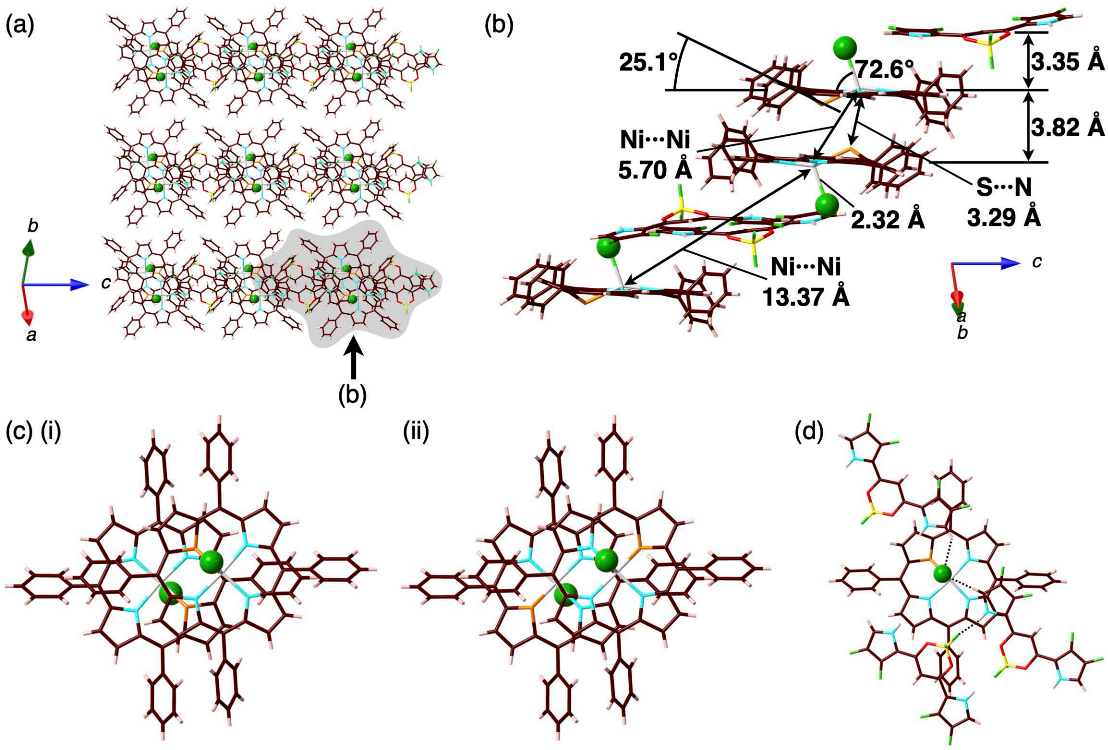

Fig. S20 Packing diagram (stacking assembly) of **1ni**$^+$-**2c**·Cl$^-$ as (a) a top view and (b) a side view from the arrow shown in (a), (c) top views of the dimers as (i) major (80%) and (ii) minor (20%) structures (Fig. S12), and (d) the enlarged structure. The stacking distance between two **1ni**$^+$-Cl$^-$ (core 25 atoms), that between **1ni**$^+$-Cl$^-$ and **2c**, and the Ni···Ni distances in the column are 3.82, 3.35, and 5.70/13.37 Å, respectively. Two pyrrole-α-CH interacts with Cl$^-$ with the C(–H)···Cl$^-$ distances of 3.41/3.85 Å, respectively. Pyrrole NH interacts with F with the N(–H)···F distance of 2.86 Å. The Ni–Cl$^-$ distance is 2.32 Å and the angle of the line through Ni and Cl$^-$ to the core porphyrin plane (25 atoms) is 72.6°. The S···N distance in two stacking **1ni**$^+$-Cl$^-$ units is 3.29 Å and the dihedral angle between the thiophene plane and the core porphyrin plane (core 25 atoms) is 25.1°. Mean-plane deviation of the **1ni**$^+$ core part (25 atoms) and τ_4 value[S11] are 0.21 Å and 0.34, respectively. Atom color code: brown, pink, yellow, blue, red, yellow green, orange, green, and light gray refer to carbon, hydrogen, boron, nitrogen, oxygen, fluorine, sulfur, chlorine, and nickel, respectively. Solvent molecules are omitted for clarity.

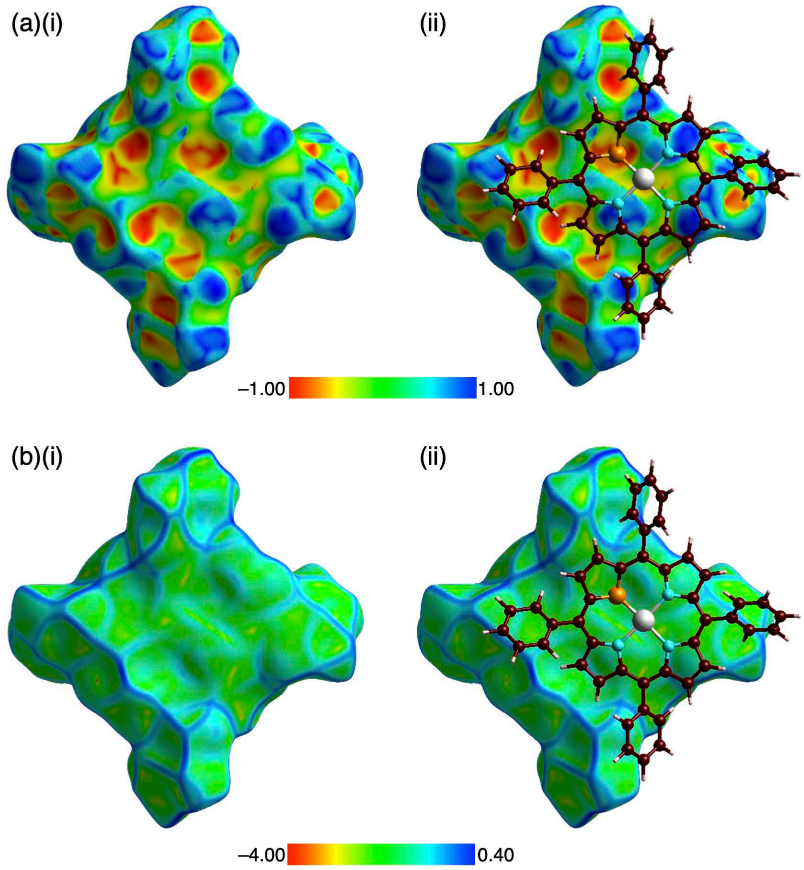

Fig. S21 Hirshfeld surface[S12] of **1ni**$^{+}$ in the crystal structure of **1ni**$^{+}$-PF_6^{-} (a major disordered structure) mapped over (a) shape-index property and (b) curvedness property: (i) only surface and (ii) surface with a ball-and-stick model of the neighboring **1ni**$^{+}$. Shape index is a qualitative measure of shape and is sensitive to subtle changes in surface shape, particularly in a flat region by differing by sign represent complementary bumps (blue) and hollows (red), whereas curvedness is a function of the root-mean-square curvature of the surface, and maps of curvedness typically show large regions of green (relatively flat) separated by dark blue edges (large positive curvature). The flat region on the curvedness surface suggested the characteristic mapping pattern for stacking in dimeric **1ni**$^{+}$. Atom color code: brown, pink, blue, orange, and light gray refer to carbon, hydrogen, nitrogen, sulfur, and nickel, respectively.

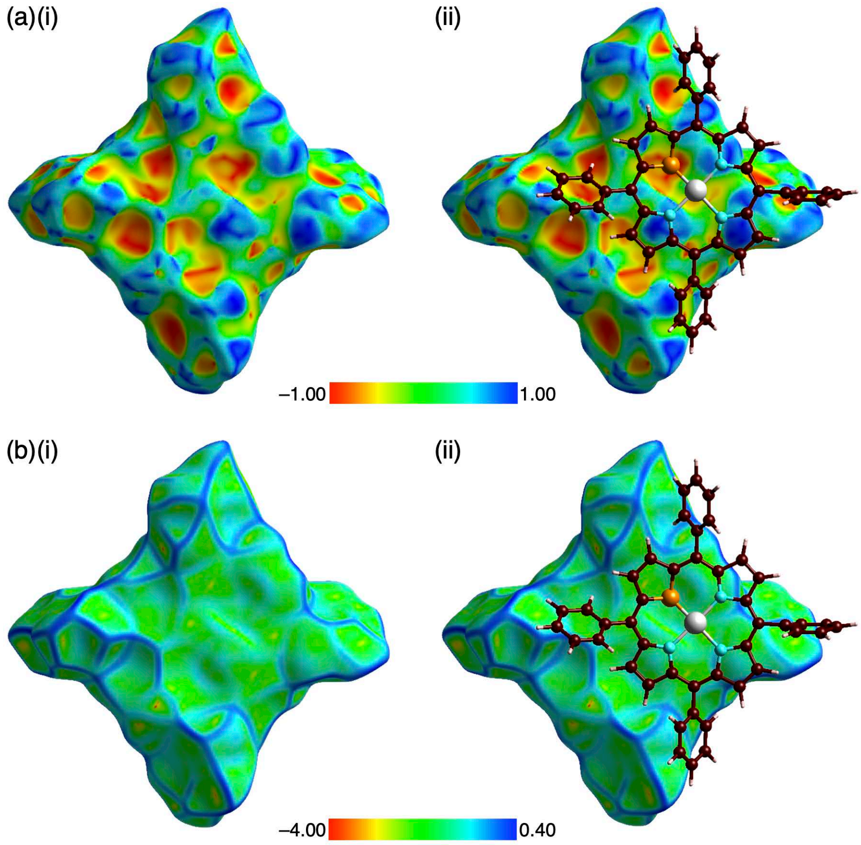

Fig. S22 Hirshfeld surface[S12] of **1ni**$^+$ in the crystal structure of **1ni**$^+$-$B(C_6F_5)_4^-$ (a major disordered structure) mapped over (a) shape-index property and (b) curvedness property: (i) only surface and (ii) surface with a ball-and-stick model of the neighboring **1ni**$^+$. Shape index is a qualitative measure of shape and is sensitive to subtle changes in surface shape, particularly in a flat region by differing by sign represent complementary bumps (blue) and hollows (red), whereas curvedness is a function of the root-mean-square curvature of the surface, and maps of curvedness typically show large regions of green (relatively flat) separated by dark blue edges (large positive curvature). The flat region on the curvedness surface suggested the characteristic mapping pattern for stacking in dimeric **1ni**$^+$. Atom color code: brown, pink, blue, orange, and light gray refer to carbon, hydrogen, nitrogen, sulfur, and nickel, respectively.

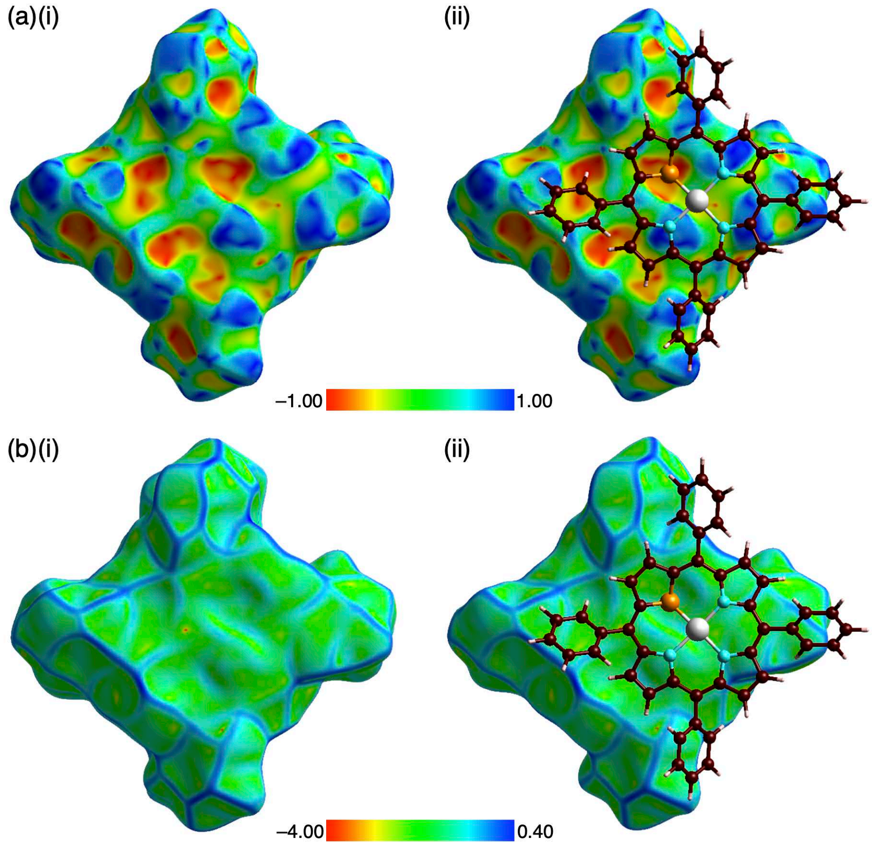

Fig. S23 Hirshfeld surface[S12] of **1ni**$^+$ in the crystal structure of **1ni**$^+$-PCCp$^-$ (a major disordered structure) mapped over (a) shape-index property and (b) curvedness property: (i) only surface and (ii) surface with a ball-and-stick model of the neighboring **1ni**$^+$. Shape index is a qualitative measure of shape and is sensitive to subtle changes in surface shape, particularly in a flat region by differing by sign represent complementary bumps (blue) and hollows (red), whereas curvedness is a function of the root-mean-square curvature of the surface, and maps of curvedness typically show large regions of green (relatively flat) separated by dark blue edges (large positive curvature). The flat region on the curvedness surface suggested the characteristic mapping pattern for stacking in dimeric **1ni**$^+$. Atom color code: brown, pink, blue, orange, and light gray refer to carbon, hydrogen, nitrogen, sulfur, and nickel, respectively.

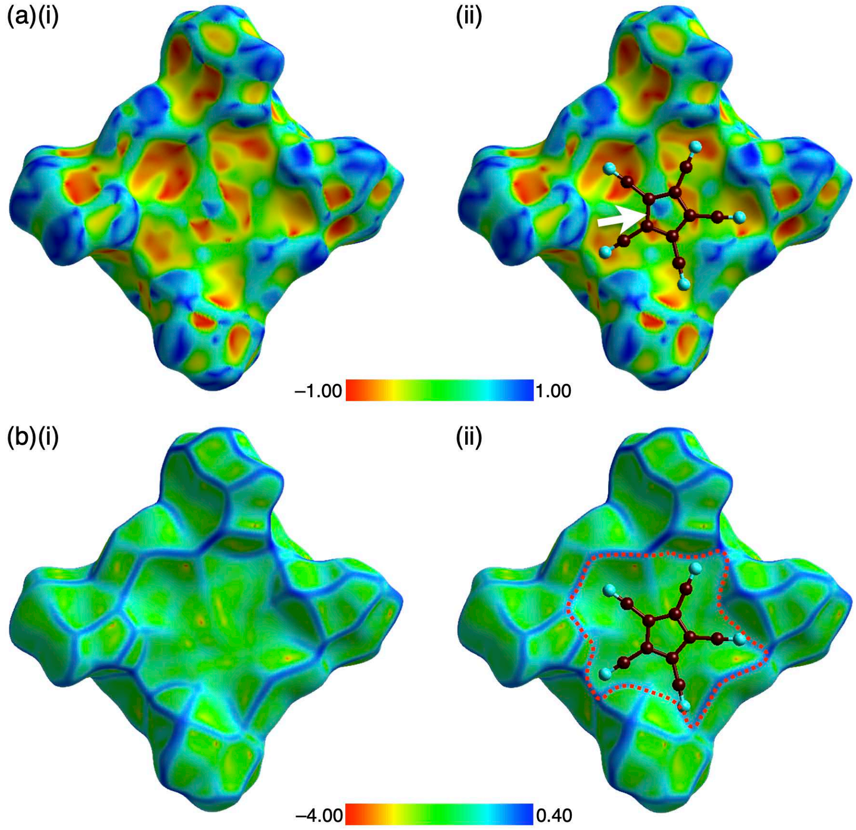

Fig. S24 Hirshfeld surface[S12] of **1ni**$^+$ in the crystal structure of **1ni**$^+$-PCCp$^-$ (a major disordered structure) mapped over (a) shape-index property and (b) curvedness property: (i) only surface and (ii) surface with a ball-and-stick model of the neighboring PCCp$^-$. Shape index is a qualitative measure of shape and is sensitive to subtle changes in surface shape, particularly in a flat region by differing by sign represent complementary bumps (blue) and hollows (red), whereas curvedness is a function of the root-mean-square curvature of the surface, and maps of curvedness typically show large regions of green (relatively flat) separated by dark blue edges (large positive curvature). The surfaces of **1ni**$^+$ showed the red and blue triangles arranged in bow-tie shapes (indicated by a white arrow in (a)) on the shape-index surface and flat region (indicated by red dashed area in (b)) on the curvedness surface, indicating the characteristic mapping pattern for $^i\pi$–$^i\pi$ stacking.[S13] Atom color code: brown and blue refer to carbon and nitrogen, respectively.

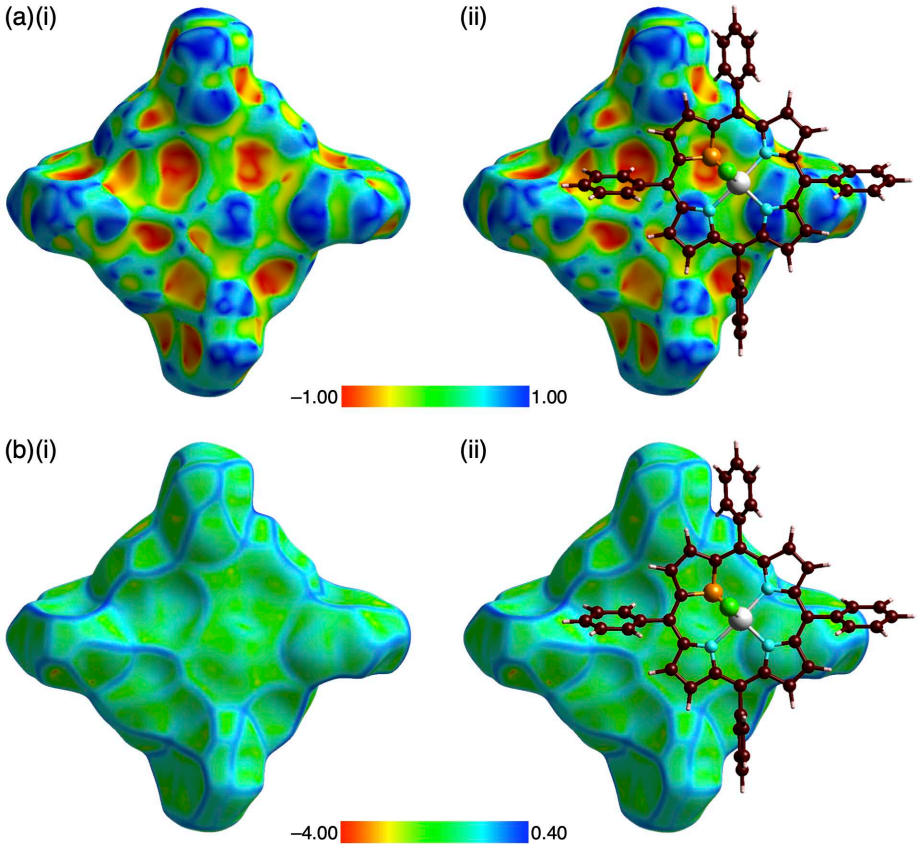

Fig. S25 Hirshfeld surface[S12] of **1ni**$^+$-Cl$^-$ in the crystal structure of **1ni**$^+$-**2a**·Cl$^-$ mapped over (a) shape-index property and (b) curvedness property: (i) only surface and (ii) surface with a ball-and-stick model of the neighboring **1ni**$^+$-Cl$^-$. Shape index is a qualitative measure of shape and is sensitive to subtle changes in surface shape, particularly in a flat region by differing by sign represent complementary bumps (blue) and hollows (red), whereas curvedness is a function of the root-mean-square curvature of the surface, and maps of curvedness typically show large regions of green (relatively flat) separated by dark blue edges (large positive curvature). The flat region on the curvedness surface suggested the characteristic mapping pattern for stacking in dimeric **1ni**$^+$. Atom color code: brown, pink, blue, orange, green, and light gray refer to carbon, hydrogen, nitrogen, sulfur, chlorine, and nickel, respectively.

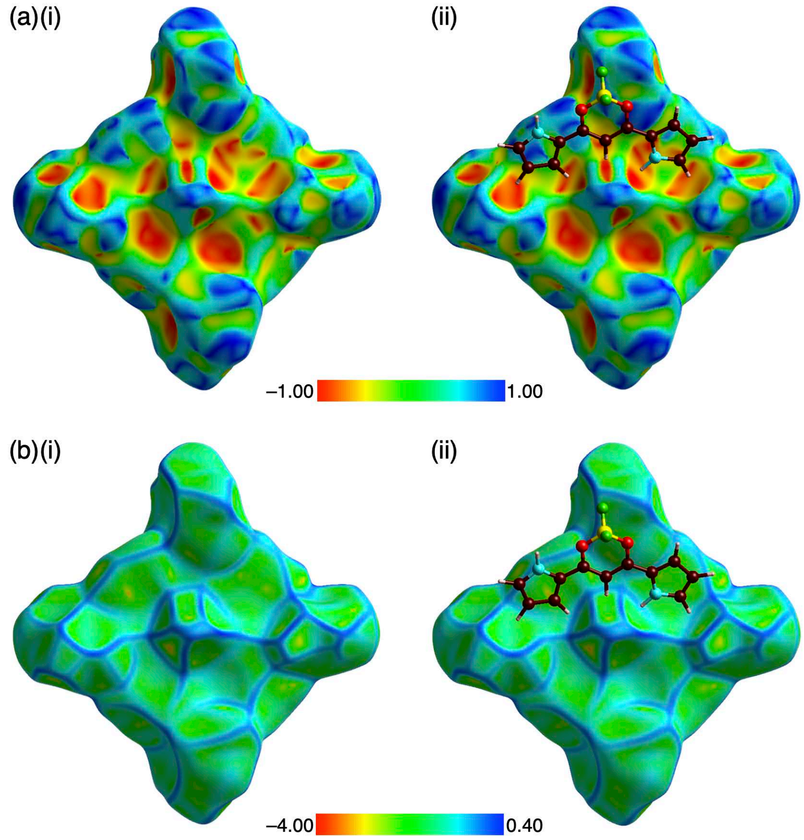

Fig. S26 Hirshfeld surface[S12] of **1ni**$^{+}$-Cl^{-} in the crystal structure of **1ni**$^{+}$-**2a**·Cl^{-} mapped over (a) shape-index property and (b) curvedness property: (i) only surface and (ii) surface with a ball-and-stick model of the neighboring **2a**. Shape index is a qualitative measure of shape and is sensitive to subtle changes in surface shape, particularly in a flat region by differing by sign represent complementary bumps (blue) and hollows (red), whereas curvedness is a function of the root-mean-square curvature of the surface, and maps of curvedness typically show large regions of green (relatively flat) separated by dark blue edges (large positive curvature). Atom color code: brown, pink, yellow, blue, red, and yellow green refer to carbon, hydrogen, boron, nitrogen, oxygen, and fluorine, respectively.

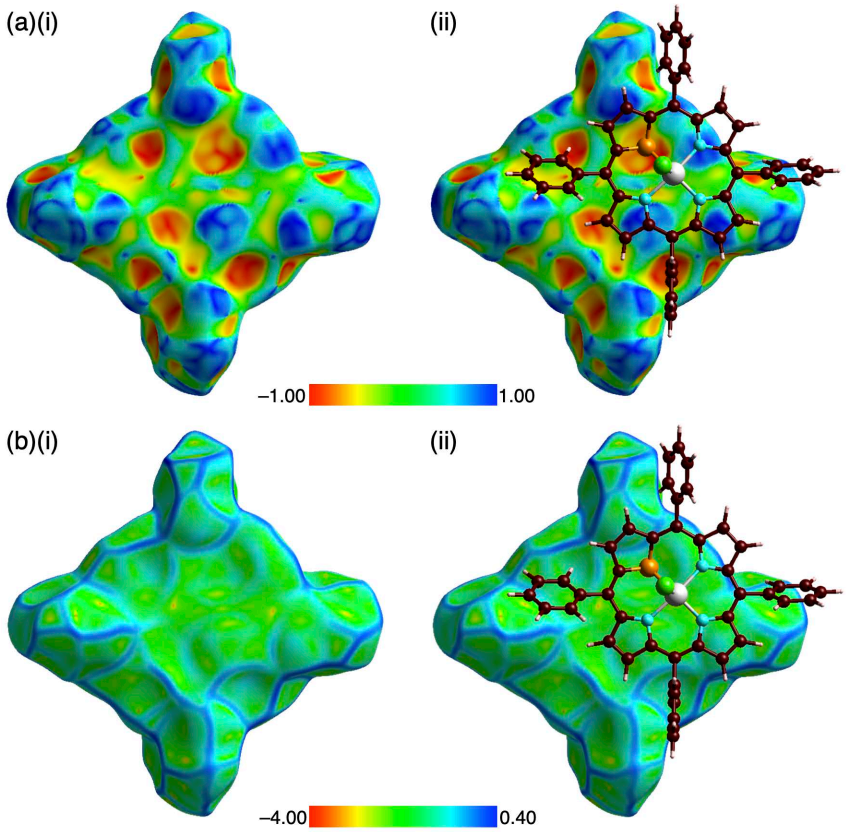

Fig. S27 Hirshfeld surface[S12] of **1ni**$^{+}$ in the crystal structure of **1ni**$^{+}$-**2b**·Cl^{-} mapped over (a) shape-index property and (b) curvedness property: (i) only surface and (ii) surface with a ball-and-stick model of the neighboring **1ni**$^{+}$-Cl^{-}. Shape index is a qualitative measure of shape and is sensitive to subtle changes in surface shape, particularly in a flat region by differing by sign represent complementary bumps (blue) and hollows (red), whereas curvedness is a function of the root-mean-square curvature of the surface, and maps of curvedness typically show large regions of green (relatively flat) separated by dark blue edges (large positive curvature). The flat region on the curvedness surface suggested the characteristic mapping pattern for stacking in dimeric **1ni**$^{+}$. Atom color code: brown, pink, blue, orange, green, and light gray refer to carbon, hydrogen, nitrogen, sulfur, chlorine, and nickel, respectively.

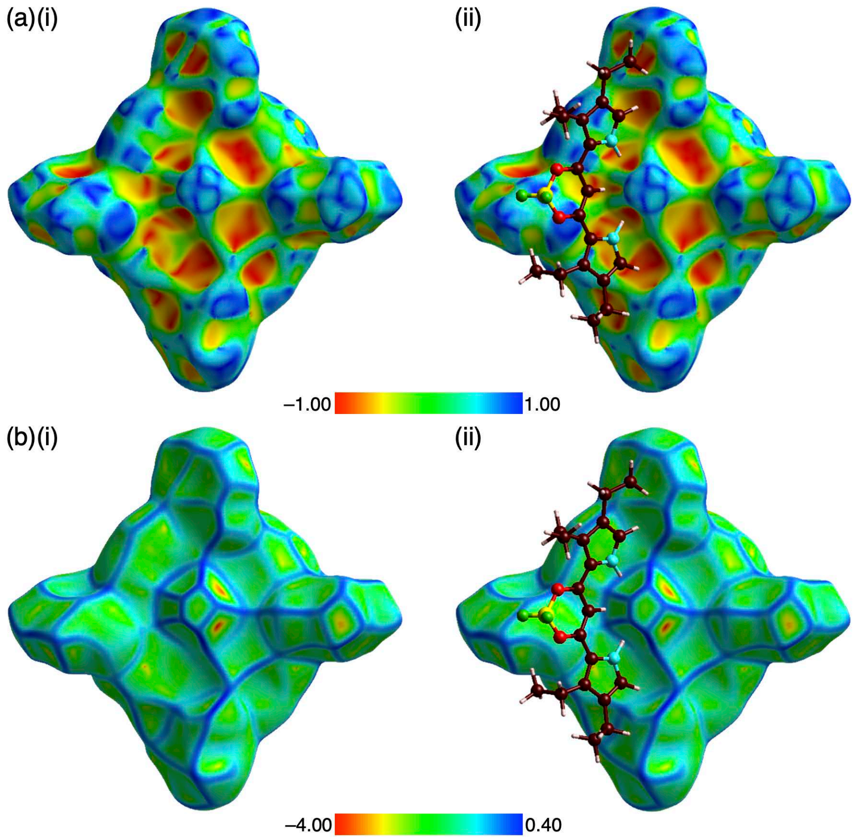

Fig. S28 Hirshfeld surface[S12] of **1ni**$^+$ in the crystal structure of **1ni**$^+$-**2b**·Cl$^-$ mapped over (a) shape-index property and (b) curvedness property: (i) only surface and (ii) surface with a ball-and-stick model of the neighboring **2b**. Shape index is a qualitative measure of shape and is sensitive to subtle changes in surface shape, particularly in a flat region by differing by sign represent complementary bumps (blue) and hollows (red), whereas curvedness is a function of the root-mean-square curvature of the surface, and maps of curvedness typically show large regions of green (relatively flat) separated by dark blue edges (large positive curvature). Atom color code: brown, pink, yellow, blue, red, and yellow green refer to carbon, hydrogen, boron, nitrogen, oxygen, and fluorine, respectively.

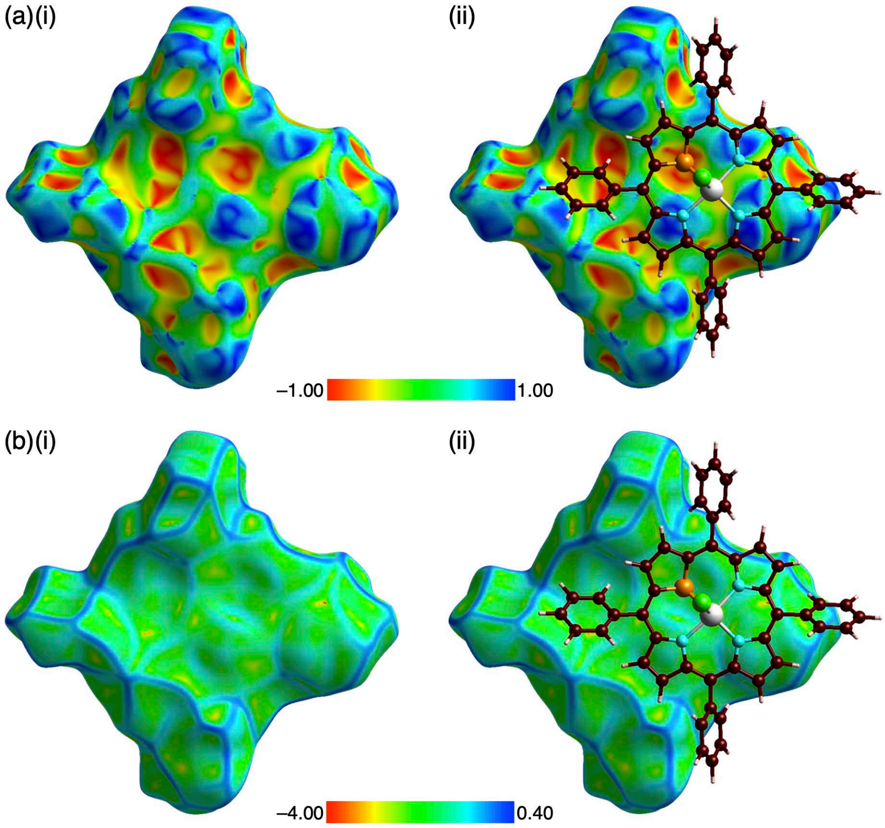

Fig. S29 Hirshfeld surface[S12] of **1ni**$^+$ in the crystal structure of **1ni**$^+$-**2c**·Cl^- mapped over (a) shape-index property and (b) curvedness property: (i) only surface and (ii) surface with a ball-and-stick model of the neighboring **1ni**$^+$-Cl^-. Shape index is a qualitative measure of shape and is sensitive to subtle changes in surface shape, particularly in a flat region by differing by sign represent complementary bumps (blue) and hollows (red), whereas curvedness is a function of the root-mean-square curvature of the surface, and maps of curvedness typically show large regions of green (relatively flat) separated by dark blue edges (large positive curvature). The flat region on the curvedness surface suggested the characteristic mapping pattern for stacking in dimeric **1ni**$^+$. Atom color code: brown, pink, blue, orange, green, and light gray refer to carbon, hydrogen, nitrogen, sulfur, chlorine, and nickel, respectively.

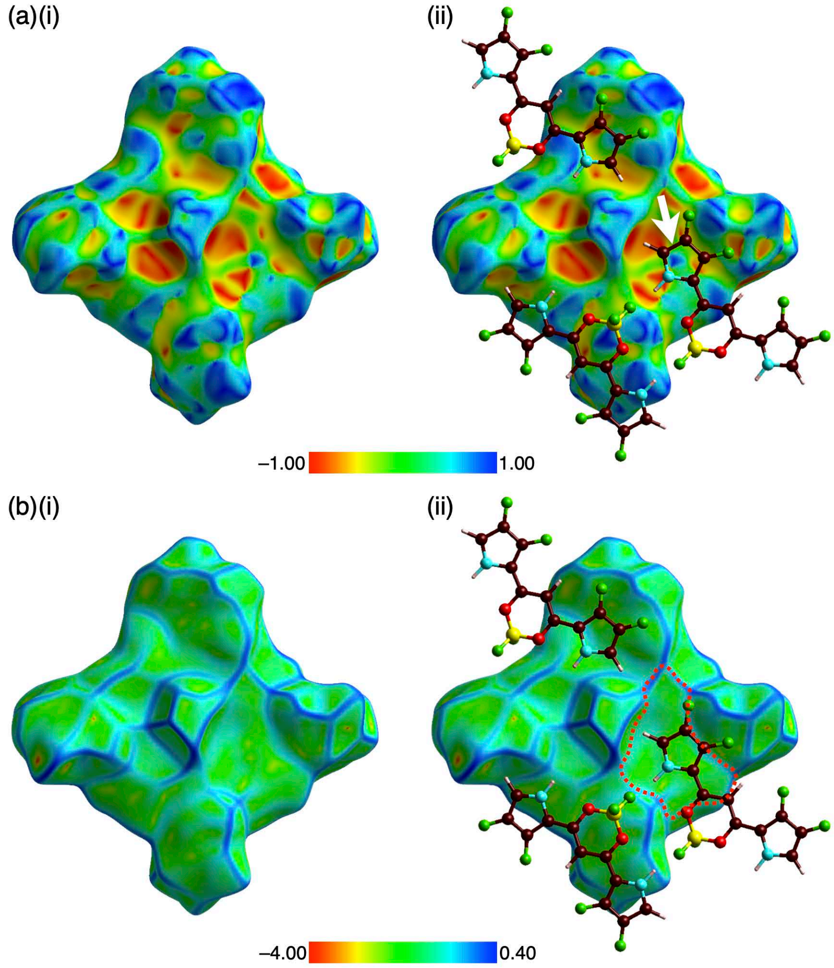

Fig. S30 Hirshfeld surface[S12] of **1ni**$^{+}$ in the crystal structure of **1ni**$^{+}$-**2c**·Cl^{-} mapped over (a) shape-index property and (b) curvedness property: (i) only surface and (ii) surface with a ball-and-stick model of the neighboring **1ni**$^{+}$-Cl^{-}. Shape index is a qualitative measure of shape and is sensitive to subtle changes in surface shape, particularly in a flat region by differing by sign represent complementary bumps (blue) and hollows (red), whereas curvedness is a function of the root-mean-square curvature of the surface, and maps of curvedness typically show large regions of green (relatively flat) separated by dark blue edges (large positive curvature). The surfaces of **1ni**$^{+}$ showed the red and blue triangles arranged in bow-tie shapes (indicated by a white arrow in (a)) on the shape-index surface and flat region (indicated by red dashed area in (b)) on the curvedness surface, suggesting the characteristic mapping pattern for stacking between **1ni**$^{+}$ and **2c**. Atom color code: brown, pink, yellow, blue, red, and yellow green refer to carbon, hydrogen, boron, nitrogen, oxygen, and fluorine, respectively.

[S4] H. Maeda, Y. Kusunose, Y. Mihashi and T. Mizoguchi, *J. Org. Chem.*, 2007, **72**, 2612–2616.
[S5] H. Maeda and Y. Kusunose, *Chem. Eur. J.*, 2005, **11**, 5661–5666.
[S6] H. Maeda and Y. Ito, *Inorg. Chem.*, 2006, **45**, 8205–8210.
[S7] K. Sugimoto, H. Ohsumi, S. Aoyagi, E. Nishibori, C. Moriyoshi, Y. Kuroiwa, H. Sawa and M. Takata, *AIP Conf. Proc.*, 2010, **1234**, 887–890.
[S8] (a) N. Yasuda, H. Murayama, Y. Fukuyama, J. E. Kim, S. Kimura, K. Toriumi, Y. Tanaka, Y. Moritomo, Y. Kuroiwa, K. Kato, H. Tanaka and M. Takata, *J. Synchrotron Rad.*, 2009, **16**, 352–357; (b) N. Yasuda, Y. Fukuyama, K. Toriumi, S. Kimura and M. Takata, *AIP Conf. Proc.*, 2010, **1234**, 147–150.
[S9] G. M. Sheldrick, *Acta Crystallogr. Sect. A*, 2008, **64**, 112–122.
[S10] (a) *Yadokari-XG*, *Software for Crystal Structure Analyses*, K. Wakita, 2001; (b) C. Kabuto, S. Akine, T. Nemoto and E. Kwon, *J. Cryst. Soc. Jpn.*, 2009, **51**, 218–224.
[S11] L. Yang, D. R. Powell and R. P. Houser, *Dalton Trans.*, 2007, 955–964.
[S12] P. R. Spackman, M. J. Turner, J. J. McKinnon, S. K. Wolff, D. J. Grimwood, D. Jayatilaka and M. A. Spackman, *J. Appl. Cryst.*, 2021, **54**, 1006–1011.
[S13] Y. Sasano, H. Tanaka, Y. Haketa, Y. Kobayashi, Y. Ishibashi, T. Morimoto, R. Sato, Y. Shigeta, N. Yasuda, T. Asahi and H. Maeda, *Chem. Sci.*, 2021, **12**, 9645–9657.

3. Theoretical studies

DFT calculations. DFT calculations were carried out using *Gaussian 16* program.[S14]

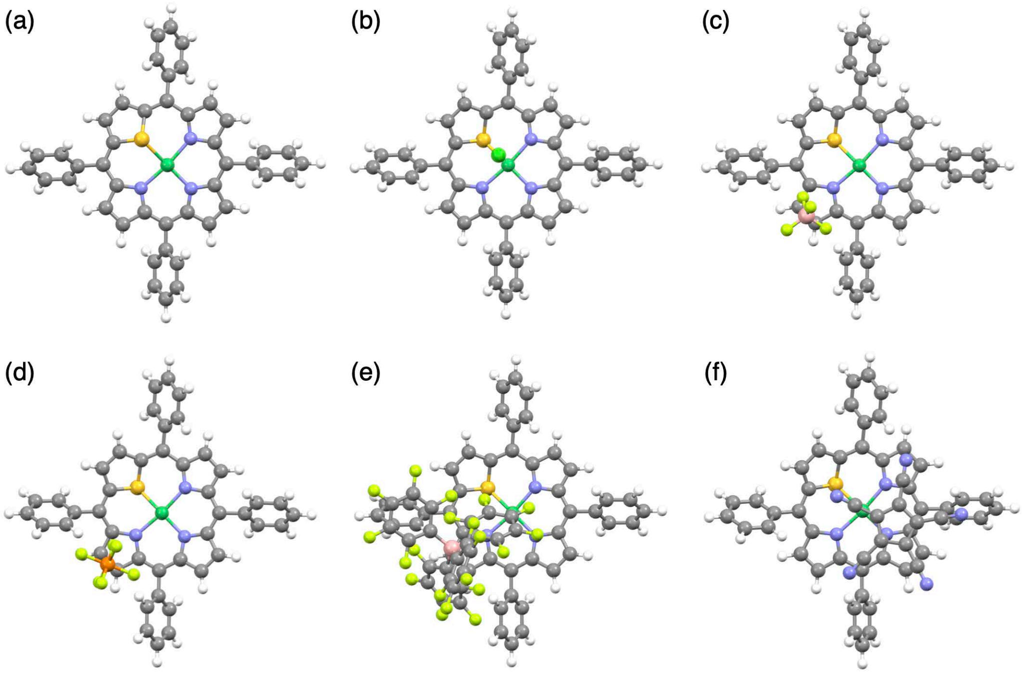

Fig. S31 Optimized structures of (a) **1ni**$^+$, (b) **1ni**$^+$-Cl^-, (c) **1ni**$^+$-BF_4^-, (d) **1ni**$^+$-PF_6^-, (e) **1ni**$^+$-$B(C_6F_5)_4^-$, and (f) **1ni**$^+$-$PCCp^-$ at PCM-B3LYP/6-31+G(d,p)(CH_2Cl_2) except for (e) at PCM-B3LYP/6-31+G(d,p)(CH_2Cl_2)//PCM-B3LYP/6-31G(d,p)(CH_2Cl_2). Crystal structures (Fig. S13,15–17) were used for the initial structures for the optimizations except for **1ni**$^+$-BF_4^-, whose initial structure was prepared based on the geometry of **1ni**$^+$-PF_6^-.

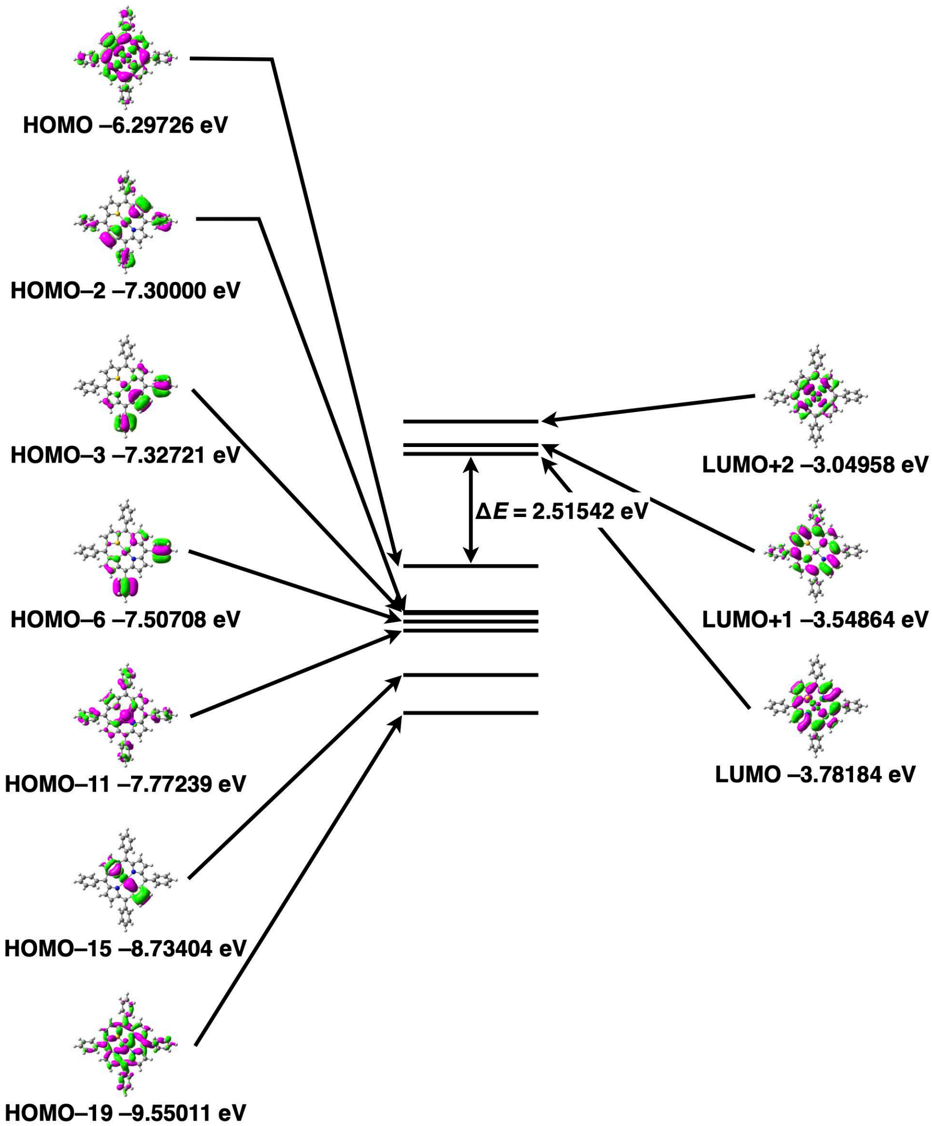

Fig. S32 Molecular orbitals (HOMO/LUMO) of **1ni**$^+$ estimated at PCM-B3LYP/6-31+G(d,p)(CH_2Cl_2).

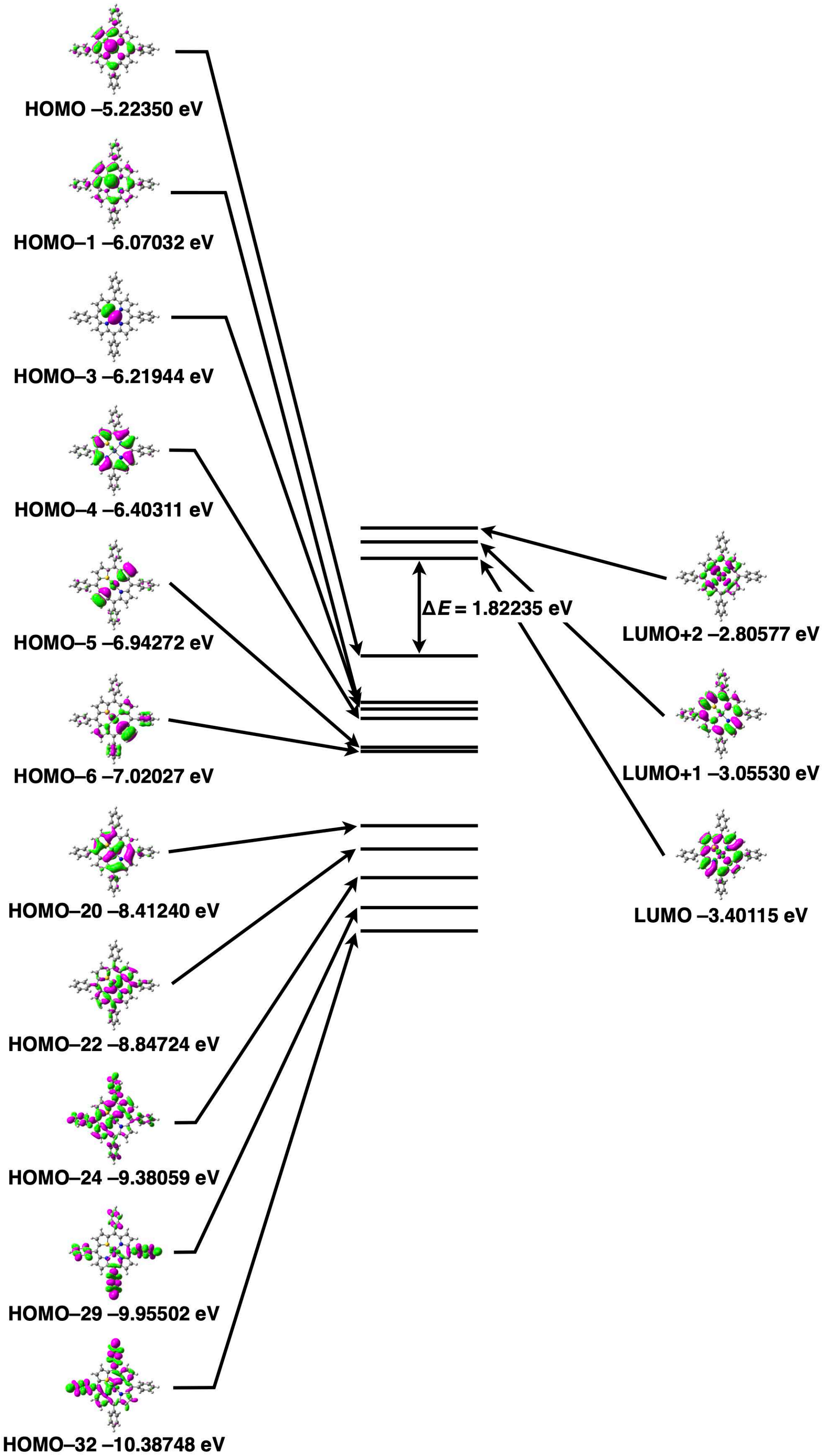

Fig. S33 Molecular orbitals (HOMO/LUMO) of **1ni**$^{+}$-Cl^{-} estimated at PCM-B3LYP/6-31+G(d,p)(CH_2Cl_2).

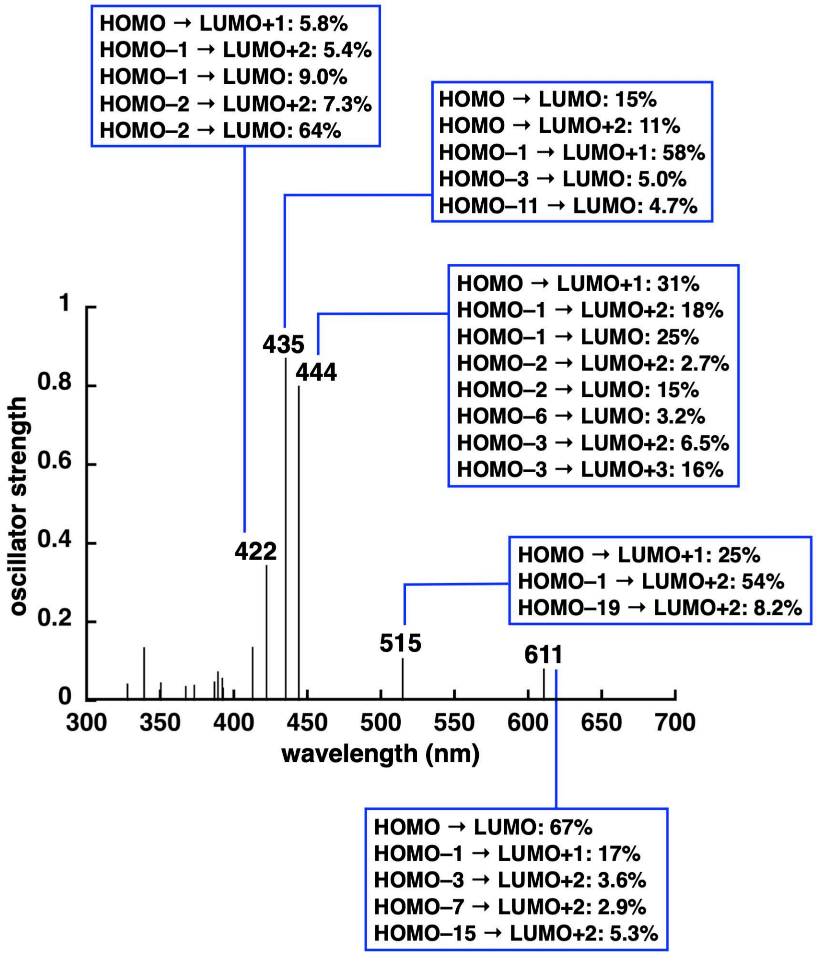

Fig. S34 TD-DFT-based UV/vis absorption stick spectrum of **1ni**$^{+}$ with the transitions correlated with molecular orbitals estimated at PCM-B3LYP/6-31+G(d,p)(CH_2Cl_2).

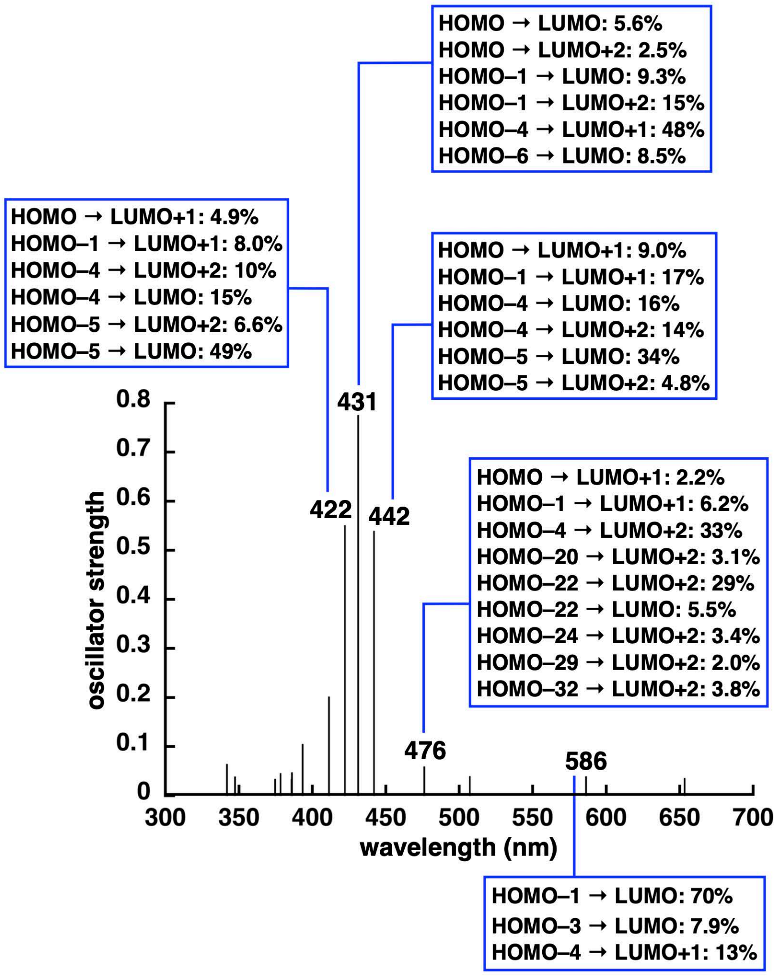

Fig. S35 TD-DFT-based UV/vis absorption stick spectrum of **1ni**$^+$-Cl$^-$ with the transitions correlated with molecular orbitals estimated at PCM-B3LYP/6-31+G(d,p)(CH_2Cl_2). Theoretical study showed a small band with the maximum at 476 nm, which was not seen in anion-free **1ni**$^+$ (Fig. S34) and may be characteristic to the Cl$^-$-coordination state.

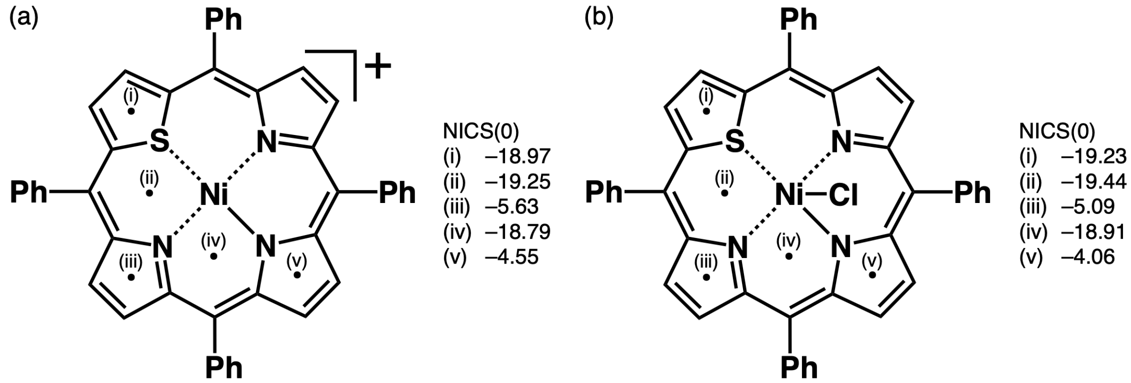

Fig. S36 NICS values (ppm)[S15] of (a) **1ni**$^+$ and (b) **1ni**$^+$-Cl$^-$ based on the optimized structures at PCM-B3LYP/6-31+G(d,p)(CH_2Cl_2) (Fig. S31). The aromaticity of **1ni**$^+$-Cl$^-$ is comparable to that of **1ni**$^+$ although the details were not discussed from the broad ^{1}H NMR signals of **1ni**$^+$-Cl$^-$ due to the paramagnetic property.

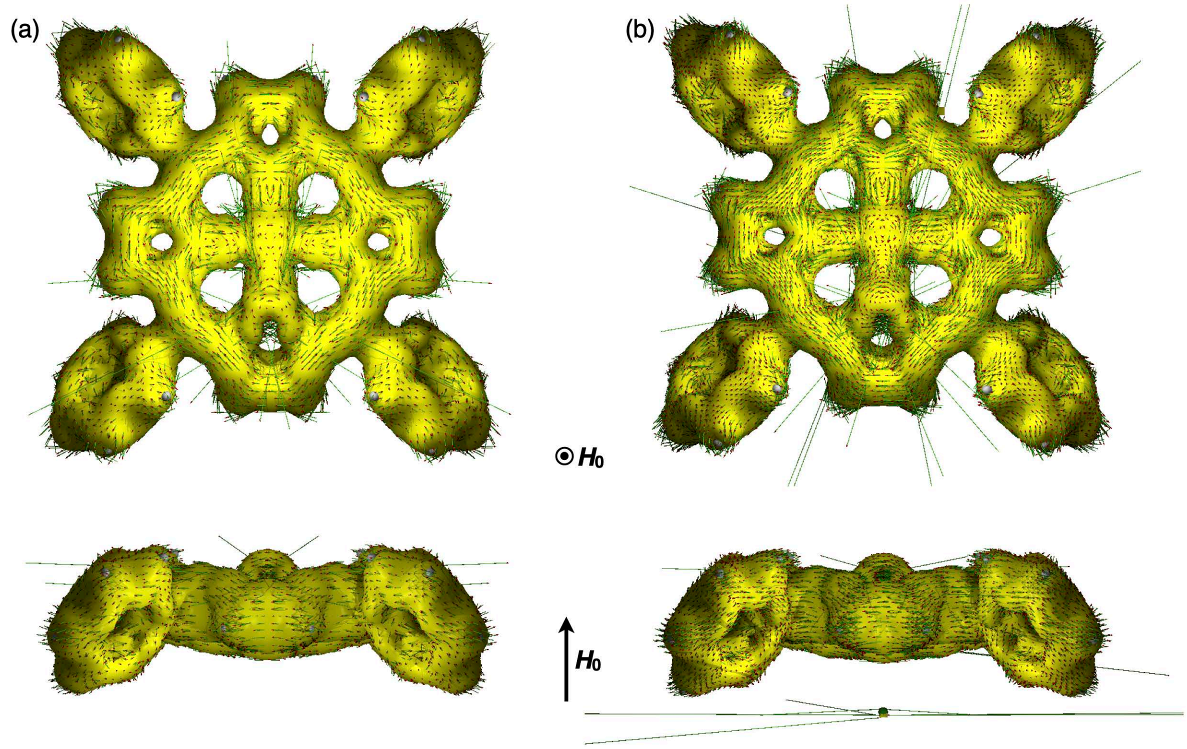

Fig. S37 Anisotropy of the induced current density (ACID)[S16] of (a) **1ni**$^+$ and (b) **1ni**$^+$-Cl$^-$ (top and side views) at isosurface value of δ = 0.015 based on the optimized structures (Fig. S31) at PCM-B3LYP/6-31+G(d,p)(CH_2Cl_2). Current density vectors are plotted on to the ACID isosurface based on the vector of the magnetic field (H_0) which is orthogonal with respect to the molecule. The theoretical results were consistent with the NICS values (Fig. S36).

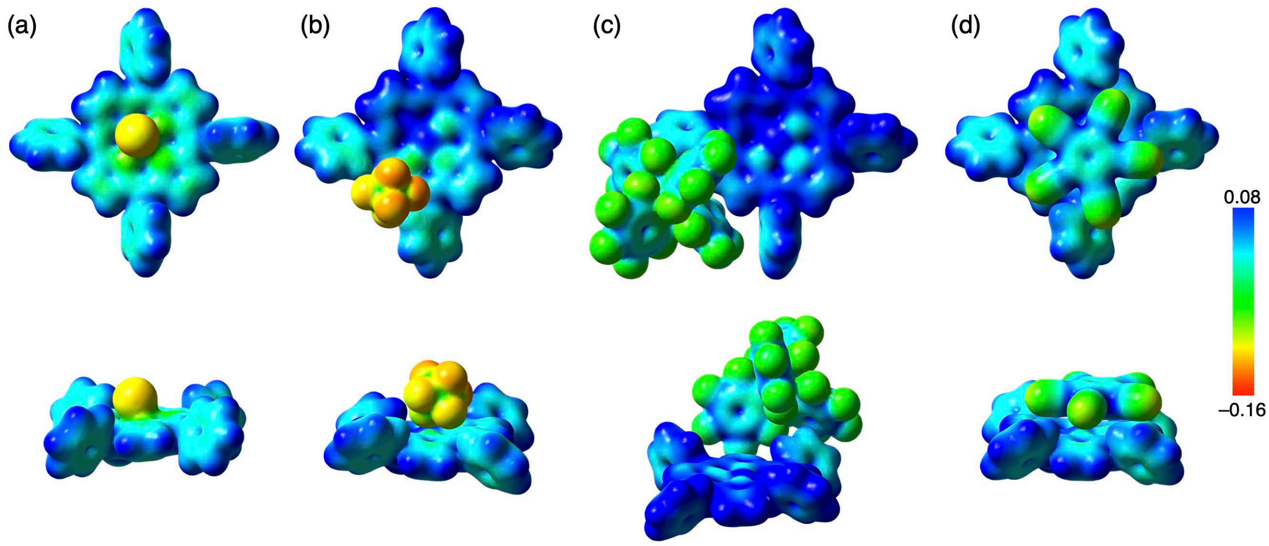

Fig. S38 Electrostatic potential (ESP) mapping (top and side views, δ = 0.01) of (a) **1ni**$^+$-Cl$^-_{tri}$, (b) **1ni**$^+$-PF_6^-, (c) **1ni**$^+$-$B(C_6F_5)_4^-$, and (d) **1ni**$^+$-PCCp$^-$ in the single-crystal X-ray structures (Fig. S13,15–17) calculated at B3LYP/6-31+G(d,p) for C, H, B, N, F, P, S, and Cl and B3LYP/LanL2DZ for Ni.

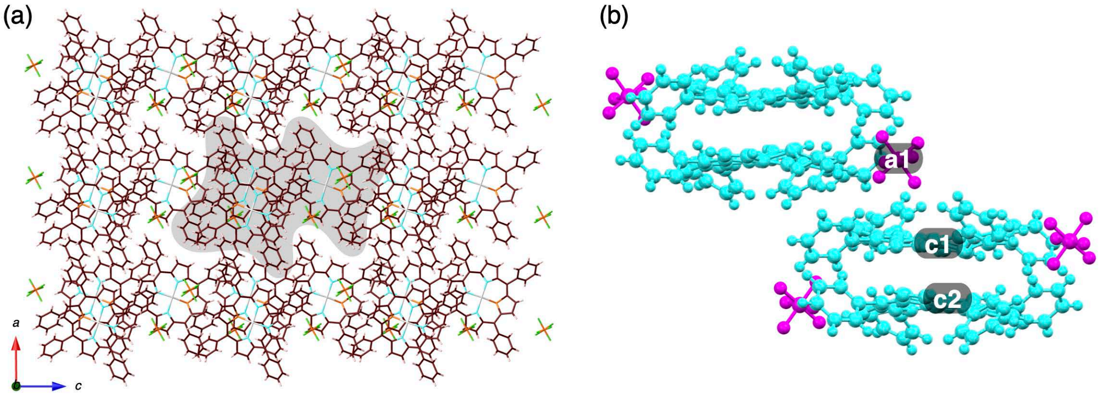

Fig. S39 Single-crystal X-ray structure of **1ni**$^{+}$-PF_6^{-} for the EDA calculations (Table S2): (a) top view of charge-by-charge structure and (b) side view of shaded part in (a). The labels (c1,2 and a1) correspond to the fragments shown in Table S2.

Table S2 Energies between selected fragments in **1ni**$^{+}$-PF_6^{-} (Fig. S39) estimated by EDA calculations based on an FMO2-MP2 using mixed basis sets including NOSeC-V-TZP with MCP for Ni and NOSeC-V-DZP with MCP for the other atoms.[S17–19]

fragments	total interaction energy (E_{tot}) (kcal/mol)	electrostatic interaction energy (E_{es}) (kcal/mol)	dispersion interaction energy (E_{disp}) (kcal/mol)	exchange repulsion interaction energy (E_{ex}) (kcal/mol)	charge-transfer interaction energy (E_{ct+mix}) (kcal/mol)
c1-c2	–160.909	0.585	–202.705	68.376	–27.165
c1-a1	–74.524	–57.149	–17.176	2.076	–2.274

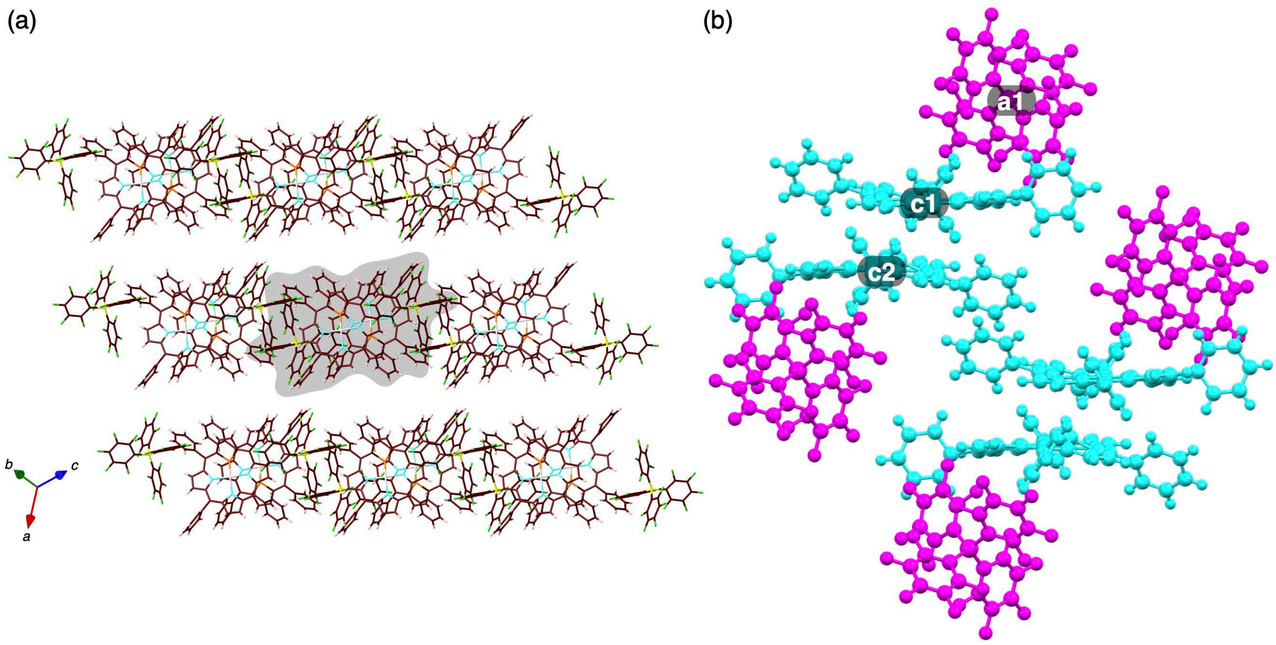

Fig. S40 Single-crystal X-ray structure of **1ni**$^{+}$-$B(C_6F_5)_4^{-}$ for the EDA calculations (Table S3): (a) top view of charge-by-charge structure and (b) side view of shaded part in (a). The labels (c1,2 and a1) correspond to the fragments shown in Table S3.

Table S3 Energies between selected fragments in **1ni**$^{+}$-$B(C_6F_5)_4^{-}$ (Fig. S40) estimated by EDA calculations based on an FMO2-MP2 using mixed basis sets including NOSeC-V-TZP with MCP for Ni and NOSeC-V-DZP with MCP for the other atoms.[S17–19]

fragments	total interaction energy (E_{tot}) (kcal/mol)	electrostatic interaction energy (E_{es}) (kcal/mol)	dispersion interaction energy (E_{disp}) (kcal/mol)	exchange repulsion interaction energy (E_{ex}) (kcal/mol)	charge-transfer interaction energy (E_{ct+mix}) (kcal/mol)
c1-c2	–139.397	12.078	–178.494	45.088	–18.069
c1-a1	–77.894	–39.681	–40.777	6.197	–3.634

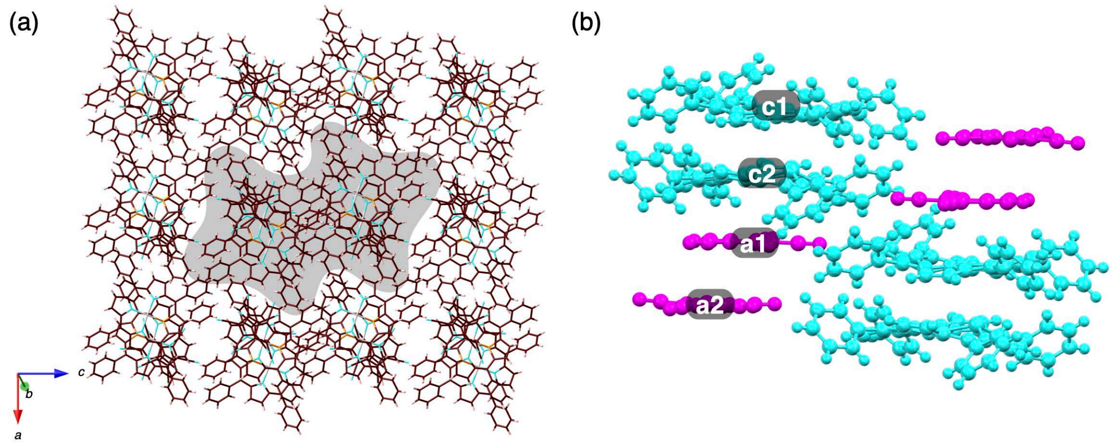

Fig. S41 Single-crystal X-ray structure of **1ni**$^+$-PCCp$^-$ for the EDA calculations (Table S4): (a) top view of charge-by-charge structure and (b) side view of shaded part in (a). The labels (c1,2 and a1,2) correspond to the fragments shown in Table S4.

Table S4 Energies between selected fragments in **1ni**$^+$-PCCp$^-$ (Fig. S41) estimated by EDA calculations based on an FMO2-MP2 using mixed basis sets including NOSeC-V-TZP with MCP for Ni and NOSeC-V-DZP with MCP for the other atoms.[S17–19]

fragments	total interaction energy (E_{tot}) (kcal/mol)	electrostatic interaction energy (E_{es}) (kcal/mol)	dispersion interaction energy (E_{disp}) (kcal/mol)	exchange repulsion interaction energy (E_{ex}) (kcal/mol)	charge-transfer interaction energy (E_{ct+mix}) (kcal/mol)
c1-c2	–145.015	14.676	–185.254	42.901	–17.338
c2-a1	–163.833	–61.142	–115.234	22.515	–9.972
a1-a2	–0.379	45.185	–52.509	10.815	–3.870

Cartesian coordination of optimized structures

Cartesian Coordination of 1ni$^+$

–2425.2657623 hartree
H,33.1395536108,15.0036693587,8.4034294974
H,34.1972122927,16.8122291573,9.7474729621
C,19.4329552759,15.8879527997,3.9540824968
C,19.0795124479,16.6662728706,2.847126063
C,19.9984305651,17.578549484,2.3183343044
H,18.7267436608,15.1738450038,4.3673358227
H,18.0955198313,16.5623707933,2.39952221
H,19.7300792898,18.1890719496,1.4611901461
C,32.6342537556,15.9566692876,8.5287001487
H,30.1480320563,13.5085965964,0.4853024588
H,29.1205882535,14.2275946598,2.620845093
H,30.9290841131,15.3672210179,7.3524057058
C,28.5742199621,16.3284734331,-0.5961748307
C,29.35414396,15.1684656886,-0.644919796
H,28.4221295575,16.9221808998,-1.4927383182
H,29.8071211329,14.8551917599,-1.5808981017
C,24.5534999102,18.3084561062,9.1235411933
C,23.8399255695,18.3895858002,10.4290559929
C,24.1068184859,19.4490494674,11.315083799
C,23.4552428483,19.5225989591,12.547946322
C,22.5401513914,18.5318135336,12.9188491455
C,22.2755288963,17.4687441503,12.0486910259
C,22.916963303,17.3986482817,10.8106489286
C,23.8083436652,18.1680091271,7.9199021368
C,22.3944365215,18.4346632947,7.8844828352
C,21.9519091233,18.1109441235,6.6405649543
C,23.0886550835,17.6202357965,5.9050152995
C,22.9859899144,17.0763389298,4.6173304239
C,21.6271986613,16.9359930241,4.0064839539
C,20.6966192977,16.0255417272,4.5345249035
C,21.2670472556,17.7084614732,2.8895941737
C,24.091131882,16.6451685175,3.8694731272
C,24.0062926761,15.994044305,2.5846631927
C,25.2834475386,15.8078282864,2.1506067798
C,26.1542925554,16.3443793853,3.1682669221
C,27.5513147228,16.4105913988,3.0657774383
C,28.1818864309,15.9802744157,1.7787935882
C,27.9857556164,16.7290109778,0.6062754555
C,29.5479023032,14.4132272264,0.5161711129
C,28.9706553027,14.8190758691,1.7223030212
C,28.3828475818,16.8479405501,4.1058569708
C,29.811814374,16.9641805432,3.9696208485
C,30.30254341,17.2806270243,5.1972169531
C,29.1815510024,17.3838427987,6.0939985236
C,29.371346797,17.6052461389,7.4863610149
C,30.7145431931,17.3861308123,8.0929686831
C,31.3890219878,16.1619892374,7.9317548757
C,33.2265626668,16.9719124175,9.2874950393
C,32.5644154936,18.1929524863,9.4525271646
C,31.3136873489,18.3971005476,8.8660756439
C,28.3228089213,17.9590662265,8.3253190921
C,28.1713099335,17.8638432167,9.729587908
C,26.8722904885,18.0534576438,10.171010554
C,25.9421507622,18.3065529068,9.1343046681
H,24.8096689505,20.2252488142,11.0269050281
H,23.6607228387,20.3536508794,13.2160233683
H,22.0370525857,18.5872726138,13.8796070163
H,21.5721611431,16.6921897756,12.3341177456

H,22.7157443423,16.5661093799,10.1433889034
H,21.8243970375,18.8409449256,8.7061501664
H,20.9490891858,18.1962811142,6.2507882737
H,20.968337807,15.4164769099,5.3917973618
H,21.9770231713,18.4193685558,2.4768848601
H,23.0894541228,15.7113686791,2.0899445327
H,25.6113454888,15.343689748,1.2328335577
H,27.3822431997,17.6314597553,0.6400959278
H,30.3622376945,16.8229959227,3.052041554
H,31.3309700172,17.4535380639,5.4757630879
H,33.0212387962,18.9873256952,10.0351778232
H,30.807047809,19.3498678339,8.9888798032
H,28.990346852,17.5759403084,10.3764407289
H,26.5631288103,17.9302117281,11.201232379
N,24.2356331236,17.6989363089,6.6771950628
N,25.4080277354,16.8197858411,4.2189211277
N,27.9936968258,17.1506289634,5.40006233
Ni,26.0721229263,17.4257784804,5.9129722765
S,26.8248268551,18.570048217,7.6366175575

Cartesian Coordination of 1ni^{+}-Cl^{-}

–2885.6408336 hartree
H,25.2354673525,0.1215305543,1.5222476439
C,24.8496415621,0.9424835935,2.1194894819
C,24.9981931837,2.2618493806,1.6783609569
H,25.5067552839,2.4699259475,0.7416390703
C,18.7419178705,9.5675425446,-0.1879142975
H,18.2051832476,9.8903594589,-1.0752394914
H,20.6395248954,9.3812861915,-1.2018305619
H,24.0817787744,-0.3373684029,3.680407379
C,25.443496316,6.1073060829,10.1356043492
C,20.132132377,8.7317037639,2.1099843673
C,23.6115416858,8.3871973171,10.1517532397
C,23.6949862939,7.5230574596,9.0013750353
C,21.6649756601,11.6369166895,8.2805221138
C,21.0719229184,6.0003903665,2.3657255723
C,24.4572246304,6.3217254668,9.038309486
C,20.8730991369,8.2935136487,3.3351760911
C,21.3331990514,6.9713823995,3.3988129856
C,21.5585620312,10.1515158684,6.2917236774
C,18.7611123602,9.0303155155,2.1753122379
C,22.9083563914,9.4888422097,9.7795803135
C,22.5701423428,9.3192854074,8.388418791
C,26.3197393722,4.7215090513,11.9345273665
C,21.9398318902,10.3159055864,7.6312789785
C,25.3891937989,4.9383513057,10.9158414721
C,20.982170097,11.1907910383,5.4717700342
C,23.3392292198,4.1917986082,4.5030242714
C,20.3461416514,12.03491712,8.5551999438
C,27.3256805329,5.6624611037,12.1781024703
C,22.4442070846,5.1430081007,3.9374826011
C,25.2415349224,4.3108992712,7.66771011
C,21.0763539035,9.2380023026,4.3517346711
C,24.3650328437,5.3567894031,8.0449419164
C,26.4588793909,7.0473743318,10.38797816
C,23.8129709206,4.3043481845,5.802716694
C,21.7671229863,4.8795079257,2.6928716467
C,23.8492574792,3.0695398308,3.6645485637
C,24.9403541286,3.7366506756,6.4439740451
C,20.6833861616,10.6249136232,4.2701627056
C,20.7991433441,8.8589815267,0.8803012829
C,23.7140410949,1.7405711353,4.1046992969
C,18.0695103807,9.439704284,1.0318842309
C,27.3942738911,6.8232881096,11.4001797733
C,24.4993459679,3.3188094792,2.442379437
C,20.108652216,9.2792493385,-0.2598090614
C,24.204702152,0.684477497,3.3336277606
Cl,25.5213860861,8.079885478,5.0560263285
H,24.0243663486,8.160533835,11.1230577174
H,20.4398747473,6.1616969231,1.505832415
H,18.2350109478,8.9313668215,3.1205105786
H,22.6407339067,10.3409969162,10.3854874779
H,26.2575718185,3.8200872187,12.5371156922
H,24.6047870476,4.2091921226,10.734524669
H,19.5225963432,11.3727954503,8.3035260776
H,28.0521600966,5.4915459482,12.9671177511
H,26.1210137944,4.0623775084,8.248071972
H,26.5239694871,7.94280007,9.7778349769
H,21.8081216932,3.943923575,2.1559823825
H,25.5583838572,2.9895865186,5.9623000936
H,20.2486303902,11.098584866,3.4030135201
H,21.8614222422,8.6407793136,0.8220028311
H,23.2069306741,1.5360433013,5.043226956
H,17.0076203473,9.6589915144,1.0956439665
H,28.1787549105,7.553111428,11.5771884167
H,24.6288138211,4.3417425788,2.1030379083
N,21.6316271854,8.9809980324,5.5797446628
N,23.0159722059,8.0936376228,7.9291952071
N,22.1382498961,6.4257069417,4.381670222
Ni,22.531473113,7.3703876475,6.1147790517
S,23.0052881572,5.3801335706,6.9327574579
C,21.1462095156,14.1238537205,9.4879296789
C,20.0893268577,13.2681125084,9.1606669237
C,22.7209017057,12.5004884863,8.6158806259
C,22.4618305044,13.7381584553,9.2111344284
H,20.9459736955,15.0842127946,9.9540385589
H,20.8388527026,12.2163965285,5.7765604798
H,19.0649263287,13.5588657445,9.3747522445
H,23.7433338186,12.2063504233,8.397800923
H,23.2879169576,14.3990458392,9.4570009924

Cartesian Coordination of 1ni^{+}-BF_4^{-}

–2849.9207917 hartree
H,-0.82174837,15.5235462679,1.8909363527
H,2.923177627,15.8098976477,14.8305040434
H,4.0556688567,15.3648539452,16.9868243476
H,0.2485459186,15.7190987213,4.1162974025
C,0.0197144662,14.0243064127,6.232024118
C,-0.6275005347,13.902106131,4.8882561818
C,-0.3959320466,14.8721360809,3.898478366
C,-1.0011764166,14.7614694295,2.6438639326
C,-1.8337321895,13.6736716582,2.3603466242
C,-2.0615724621,12.7006749749,3.3388514523
C,-1.4682681911,12.8134758095,4.5997503235
C,-0.7932033583,14.273680466,7.3457123389
C,-2.2139166975,14.4886338825,7.2442573495
C,-2.6939575922,14.566966386,8.5127362533
C,-1.5739818162,14.4195602246,9.4049989192
C,-1.7627280768,14.3447162357,10.8127687097
C,-3.1222038969,14.0793669936,11.3625939956

C,-3.8551977795,12.950506445,10.9521218557
C,-5.1167190739,12.6988744997,11.4964444111
C,-5.6639600185,13.5688570472,12.4456263872
C,-4.940172079,14.6928149202,12.8582800029
C,-3.6735969624,14.9431752879,12.326262
C,-0.7030932702,14.4391119195,11.7048259382
C,-0.570689873,14.0208888787,13.0507438362
H,-2.300608254,13.5849406078,1.3836231751
H,-2.7024007471,11.8504428706,3.1241926356
H,-1.6434763994,12.0499542978,5.3527079346
H,-2.7664948975,14.562171666,6.3202956753
H,-3.7145984565,14.7219290151,8.82751204
H,-3.427647338,12.2633596958,10.2277533618
H,-5.6697048167,11.8196951897,11.1793330071
H,-6.6473741182,13.3716355966,12.8623920946
H,-5.3608510479,15.3751205409,13.5911292475
H,-3.117167113,15.820934174,12.6423417794
H,-1.412397163,13.6455017971,13.6188899964
N,-0.396139706,14.279018003,8.671714395
C,3.5723732519,14.9450813907,14.9320568149
C,4.2144198169,14.6951856389,16.1467774641
C,5.0596433008,13.5885625562,16.2795954835
C,5.2634914828,12.7349938382,15.1900411203
C,4.6312456123,12.9887227404,13.9713008012
C,3.7787321065,14.0984725867,13.8278729384
C,3.0737969225,14.3608874475,12.5411521832
C,3.821097751,14.456133948,11.3343367277
C,5.2481100344,14.6420167351,11.3547042589
C,5.6816465615,14.5951495613,10.0667787868
C,4.5251629069,14.3551826643,9.2430157364
C,4.6056816093,14.1206707949,7.8635103951
C,5.9585986944,14.0610398397,7.2259919776
C,6.8415465829,13.0075796783,7.5161889747
C,8.0988977566,12.9494907689,6.9090395942
C,8.4940318942,13.9485012029,6.0135005696
C,7.6227169644,15.0031159962,5.7222597661
C,6.3603658949,15.0562358463,6.319392631
C,3.4847175695,13.9240301156,7.0446820799
C,3.5442562004,13.5687116401,5.6474960652
C,2.2610516337,13.5347560347,5.1930751294
C,1.4120092619,13.8734810478,6.3092746085
C,0.7337174625,14.0212412694,13.5162442747
C,1.6879090109,14.4415223871,12.5584753903
H,5.5550196895,13.3918367391,17.2257815671
H,5.9113416169,11.8690972147,15.2889594625
H,4.7837152378,12.3168289784,13.1322565264
H,5.8337070579,14.8098802703,12.2458626661
H,6.6910361212,14.7111643177,9.7027353922
H,4.4491362034,13.3604243015,5.096895594
H,1.9142845526,13.2932611883,4.1998018078
H,1.0247535194,13.6468804333,14.4895332357
H,6.53682912,12.2270666644,8.2072346853
H,8.767274518,12.1240442437,7.1358649379
H,9.4729048084,13.9047427283,5.5451092638
H,7.9230684978,15.7843559136,5.0301218535
H,5.687080797,15.8774324018,6.091106612
N,2.1756801786,14.0765329738,7.4323978769
N,3.3789667403,14.3147767808,10.0189151584
Ni,1.5342932447,14.3224596485,9.222589658
S,0.836898524,15.0903795402,11.1631437585
F,-2.1482463859,8.5061700756,8.283677652
F,-1.8431412346,10.2020888787,6.7459915157
F,-2.2781300674,10.7114108178,8.9571213167
F,-3.9406013938,9.8094546809,7.6306734596
B,-2.5540474953,9.8059193797,7.9043237839

Cartesian Coordination of 1ni^{+}-PF$_6^{-}$

–3366.0600126 hartree
H,3.3679474516,6.1642557169,-3.0909040615
H,-4.4798390739,-4.6212187349,-1.3238658908
H,-6.1534073168,-6.2252178645,-0.4544740367
H,1.5963940858,4.4555680584,-2.8130874874
C,1.5241790133,2.4018911213,-1.0307419608
C,2.5967467776,3.4320428661,-1.1958090376
C,2.4718654792,4.4365514545,-2.1703078999
C,3.4725483733,5.3992695218,-2.3269487085
C,4.602652609,5.3771052351,-1.50288328
C,4.7295644494,4.3845122966,-0.5257692974
C,3.7366088782,3.4126035936,-0.3742738703
C,1.8186271766,1.0695266252,-1.3480727918
C,3.0872511713,0.6553120545,-1.8899012584
C,3.0744061094,-0.702530925,-1.9332780937
C,1.7929608723,-1.1348526156,-1.4410956453
C,1.5040829147,-2.5152344881,-1.2561087064
C,2.6174985855,-3.5045286934,-1.2265386485
C,3.6973304774,-3.3443465699,-0.3386584025
C,4.721400958,-4.2927833086,-0.2995162319
C,4.6868979075,-5.404275849,-1.1484487837
C,3.6169097084,-5.5702287925,-2.0344874094
C,2.5841506265,-4.6308535725,-2.0686037914
C,0.2127893803,-2.9728976659,-1.0314977144
C,-0.2728667293,-4.1742055867,-0.462122726
F,5.0247365416,-1.4972678783,2.682340528
F,3.0809095584,-0.5286021329,1.8468910124
F,3.5652493422,-0.3882333527,4.1194208731
F,3.6948273314,1.51463448,2.7808760252
F,5.6383462395,0.5430722148,3.621367041
F,5.1550442752,0.4067590511,1.3486512461
H,5.3782582803,6.1282036372,-1.6212494887
H,5.6014068678,4.3634251845,0.1214610236
H,3.8393970113,2.6486958283,0.3904601874
H,3.883148148,1.3209225298,-2.1866322309
H,3.8557074908,-1.3629820675,-2.2772273654
H,3.7229014175,-2.4919548699,0.3328582598
H,5.5439186288,-4.1624043136,0.3973308055
H,5.4878421962,-6.1372181715,-1.1187038628
H,3.5865522292,-6.4281104421,-2.6997739439
H,1.7586822459,-4.7580176411,-2.7631155179
H,0.3854088006,-4.9966877931,-0.2123366048
N,1.0066078008,-0.0285939079,-1.1222254812
P,4.3597586469,0.008529773,2.7335686976
C,-4.9097433226,-4.4727394792,-0.3376222546
C,-5.8564660798,-5.3749066809,0.15223893
C,-6.4210907865,-5.1823102583,1.4174326029
C,-6.0374661907,-4.0803544235,2.1892987638
C,-5.0991997183,-3.170920351,1.6974111257
C,-4.5250602604,-3.3562420323,0.4265471668
C,-3.4992654835,-2.4094277956,-0.0954921953
C,-3.7847080105,-1.0167405936,-0.1438527896
C,-5.1321366475,-0.5267946998,-0.0199158745

C,-5.0685484961,0.8311190969,0.0125300302
C,-3.6759389303,1.1882203745,-0.0703285242
C,-3.2160118871,2.5054204905,0.0663300563
C,-4.209537205,3.5813047571,0.3748132891
C,-4.8661325262,3.6148352669,1.6163678195
C,-5.7840417057,4.6281724745,1.9051225001
C,-6.0658645639,5.6135506125,0.9534188483
C,-5.4198286101,5.5851153712,-0.2867428247
C,-4.492551113,4.5794740319,-0.5724456086
C,-1.8685165956,2.8714182816,-0.0592942981
C,-1.354275185,4.1984907924,0.1779838917
C,-0.0272563861,4.1684623313,-0.1260689357
C,0.2745874303,2.8238161069,-0.5530633927
C,-1.6219852102,-4.145915971,-0.1494059172
C,-2.2601369666,-2.9206090848,-0.4579712427
H,-7.1538215256,-5.8866472006,1.8000018548
H,-6.4650932078,-3.9300188605,3.176106352
H,-4.7962757569,-2.3237877509,2.305124586
H,-6.0123582783,-1.1506582837,0.016199365
H,-5.8866327477,1.5312736497,0.0859552597
H,-1.9333845619,5.0340731248,0.5410266738
H,0.6878824451,4.974309207,-0.0597430421
H,-2.1353553824,-4.9445859704,0.3709660259
H,-4.6465138787,2.8543413938,2.3599848317
H,-6.2769586728,4.6467664615,2.8727045106
H,-6.7823477332,6.3984921737,1.1770141081
H,-5.6352854467,6.3449807924,-1.0322340298
H,-3.9937569999,4.5604359767,-1.5371382708
N,-0.8528040609,2.0441519667,-0.4731257674
N,-2.8938691713,0.0548936877,-0.2141446011
Ni,-0.9436230081,0.140979689,-0.6907141613
S,-1.1546605004,-1.9313656807,-1.401820331

Cartesian Coordination of 1ni^{+}-B(C_6F_5)$_4^{-}$

–5361.3663366 hartree

C,7.5722383704,-14.9779767834,-28.7915821051
C,6.2903253593,-15.5073293564,-28.8469181931
C,5.5400787976,-15.5709778961,-27.6776695391
F,8.3104065602,-14.8995290973,-29.9139965496
F,5.7809807947,-15.9464702834,-30.008832984
F,4.2919081481,-16.0726116409,-27.7094317892
C,7.6495672277,-14.9427144511,-23.6179478007
C,7.7654023529,-14.4356644979,-22.3193483457
C,7.7227911775,-15.2085025257,-21.1655969917
C,7.5812857479,-16.5864588736,-21.2721688961
C,7.476199022,-17.1509633278,-22.5356266859
C,7.5145432364,-16.3326249669,-23.6668010238
C,9.5217455962,-13.6931025119,-24.8193242657
C,10.1495652574,-12.5814933843,-24.2544408579
C,11.5182601885,-12.5040168413,-23.993494448
C,11.7720595495,-14.6990998936,-24.8995127356
C,10.4000737313,-14.7402584344,-25.1184406911
F,7.5640044263,-17.3574089403,-20.1705473893
F,7.3485471431,-18.483852999,-22.6619095894
F,7.4240697766,-16.9890250214,-24.8435015004
F,9.4381382422,-11.4921599718,-23.8753668304
F,9.9216560875,-15.895739178,-25.6309549634
B,7.8800439883,-13.937287966,-24.924292758
C,7.3836409033,-14.5828579509,-26.3685164269
C,8.0843620189,-14.5249394782,-27.5749461835
C,6.0922085035,-15.1062820635,-26.4891997156
C,6.9858323461,-12.5412367311,-24.8645046156
C,7.2914940241,-11.4828138334,-25.7265288858
C,6.5439138755,-10.3153190394,-25.834193192
C,5.3984149774,-10.1670614827,-25.0596287428
C,5.0343268168,-11.1943656584,-24.2002659583
C,5.8168772313,-12.347498062,-24.1256178021
F,9.332715515,-14.0107001846,-27.6385036661
F,5.2938082329,-15.1794803236,-25.3988968881
F,8.3796052926,-11.5627725846,-26.5271273371
F,6.9118728568,-9.3353543788,-26.6795762934
F,4.6566337297,-9.051277421,-25.1450660327
F,3.924746321,-11.0732291177,-23.4482967527
F,5.3599487477,-13.2908668092,-23.2719751885
C,12.3415625625,-13.5738961728,-24.3146477034
F,13.656527414,-13.5366798057,-24.0445461568
F,12.5475811664,-15.7595596499,-25.2055841269
C,8.0340560814,-22.6877206339,-16.8861621721
C,9.0937390136,-23.4294292229,-16.3589445775
H,7.0817397755,-23.1668499053,-17.0924025909
H,8.9667081554,-24.4870238041,-16.1482010664
C,7.2455185602,-15.1829399661,-15.672351412
C,11.1689099562,-13.4129419994,-19.2563153717
C,10.2667736147,-12.4301990778,-18.7658756142
C,10.2638499139,-11.0640963969,-19.3599639373
C,10.0797640182,-10.8778209415,-20.7396930691
C,10.4269264503,-9.9381969979,-18.5337597042
C,9.3379373593,-12.7077692302,-17.7735977885
C,8.1375550355,-12.0525632662,-17.4133703692
C,7.3175919073,-12.796511882,-16.5836083954
C,7.8381539935,-14.0689341081,-16.2501033305
F,7.945742769,-13.1062269215,-22.1274898719
F,7.8326860296,-14.6371401143,-19.9482290137
H,12.5151392748,-12.0291813935,-20.3864126987
H,9.9066412417,-11.7345826478,-21.3786527084
H,10.5761819814,-10.073176995,-17.4666389651
H,7.8588016079,-11.0976077187,-17.839668079
H,6.3235053894,-12.4894983593,-16.2855273373
N,8.7741158026,-16.9459524398,-16.6872125824
Ni,10.0458389763,-15.9775807842,-17.8935776158
S,9.5074289846,-14.1533895995,-16.7918091705
C,10.0757691727,-9.5941271437,-21.2837151612
C,10.2518318732,-8.4815002766,-20.4577811616
C,10.4249761591,-8.6558780516,-19.0819751154
H,9.9340915511,-9.4748428274,-22.352315411
H,10.2517348047,-7.4822849526,-20.8830504569
H,10.564634682,-7.7945192903,-18.4357471343
C,8.844277291,-18.3111154328,-16.4694879044
C,9.5997051772,-19.2385655346,-17.1995938585
C,10.5145687283,-18.8735734915,-18.1959919958
C,11.2602564262,-19.8064021566,-19.0037934037
C,12.1012901414,-19.0723151334,-19.7802589472
C,11.8642166301,-17.6865889253,-19.4613037462
C,12.5577884289,-16.6141968306,-20.037648789
C,13.7194423393,-16.9316571967,-20.9243406209
C,13.6767054278,-16.6532476749,-22.2986815429
C,14.768810302,-16.9462218891,-23.1160607842
C,15.9181812952,-17.5211415798,-22.5697584123
C,15.9686438078,-17.8077177965,-21.2032461084
C,14.8756901335,-17.519191278,-20.385034385

C,12.2156661361,-15.2717751218,-19.8276531637
C,12.9275866461,-14.1803526943,-20.4396226069
C,12.2721062305,-13.0408976638,-20.1019210081
F,12.0398709027,-11.4112464969,-23.4048901467
H,11.1459298227,-20.8789699182,-18.9781383794
H,12.80796605,-19.4260646419,-20.5150214034
H,12.7810780867,-16.2222223144,-22.7306242596
H,14.7127948829,-16.7205651471,-24.1756397599
H,16.7696005075,-17.7462403219,-23.2050750336
H,16.8598111912,-18.2534602684,-20.771563149
H,14.920375937,-17.7368448934,-19.3220498519
H,13.8040942189,-14.2788095771,-21.0606108828
N,11.1523892872,-14.7972864161,-19.0781923528
N,10.8755351092,-17.5870970594,-18.5141176232
C,7.8053992875,-16.4840749772,-15.7948651076
C,7.3282698844,-17.5713825915,-14.9834373409
C,7.9737158312,-18.6943854239,-15.3897997444
C,3.4900028005,-14.5982843599,-13.6651588822
C,5.8265012041,-14.0387881769,-13.9483534425
C,3.5960444103,-15.5494580965,-14.6832034252
C,4.8145404347,-15.751727022,-15.3298912181
C,5.9462552899,-14.9991984017,-14.9683397427
C,4.6078929888,-13.8448706391,-13.2986778786
H,6.6044489129,-17.4723275341,-14.1895080184
H,6.6963642779,-13.4597144721,-13.6535834747
H,2.7282264026,-16.1310141957,-14.9788616579
H,2.5407346464,-14.4441808172,-13.1610958838
H,4.8895740042,-16.4815517177,-16.1297356332
H,4.533251473,-13.1084886985,-12.5043426826
C,9.4227120693,-20.6931232724,-16.9045532424
C,8.1945253539,-21.3276475414,-17.1535116968
C,10.3177373879,-22.806341803,-16.1042896098
C,10.4841297052,-21.4485854139,-16.3794795545
H,7.8773677057,-19.6942946479,-14.9966525304
H,7.3710165682,-20.7549967453,-17.5691360909
H,11.1441786387,-23.3756814545,-15.6896532288
H,11.4354221331,-20.9661680051,-16.1760693101

Cartesian Coordination of 1ni^{+}-PCCp^{-}

–3080.1949264 hartree

H,0.5486854562,7.235609839,1.9562871629
H,-1.0108605299,8.833349979,0.8550021342
C,0.0365670193,-6.8922728789,0.038130353
C,0.507236203,-7.5395445688,-1.1088078111
C,0.7987296541,-6.7943011304,-2.2560403052
H,-0.1851921042,-7.462793164,0.9352443777
H,0.6476931994,-8.6164963104,-1.1082507889
H,1.1623817462,-7.2897853273,-3.151544929
C,-0.0991188309,6.8992154426,1.152281218
C,2.4265408548,-1.531016158,3.4303980564
C,3.2295675307,-2.6944534353,3.5165711793
C,1.0084094302,-1.4975449047,3.3849192113
C,0.1465886696,-2.6207532589,3.4103548474
C,0.6040685792,-0.139657407,3.3034761567
C,-0.7307362696,0.3285174338,3.2437435752
C,1.7722531979,0.6660907346,3.295577849
C,1.8069810674,2.0792005701,3.2135983639
C,2.8985356421,-0.1938781676,3.3759829244
C,4.2547503774,0.2131020655,3.4002142293
H,7.1556223413,2.0809687945,-0.4348505654
H,4.7416906876,1.7816793289,0.018585018
H,0.6217722732,4.8710943384,1.2358382159
N,3.8913930464,-3.6518087304,3.5884363247
N,-0.5644838357,-3.544967533,3.425163313
N,-1.8303126557,0.7141682952,3.1974714752
N,1.8340180912,3.2426992724,3.1381434173
N,5.3708073106,0.5503870993,3.4216733916
C,6.258057018,0.5067065066,-3.3184409321
C,7.0764590768,1.1385491268,-2.3764622143
H,6.6774062759,0.1503775343,-4.2548185226
H,8.1356797772,1.2712135111,-2.576250097
C,-3.9928656735,-0.3841653255,-0.481628706
C,-5.3675002286,-0.6806118502,0.0133469783
C,-6.4834173557,-0.1082896665,-0.6234133542
C,-7.7743037598,-0.3639167989,-0.1558537001
C,-7.9664946408,-1.181677181,0.9626000578
C,-6.8617630789,-1.7461675909,1.6093095613
C,-5.5707455834,-1.5013722272,1.1374535612
C,-3.1100646542,-1.4534545343,-0.7980870061
C,-3.5968632543,-2.8007165763,-0.9411184263
C,-2.5159490396,-3.6066245518,-1.112320098
C,-1.3507120328,-2.7618248484,-1.0645717569
C,-0.0440939115,-3.266843133,-1.1070332526
C,0.1452229391,-4.7519106197,-1.1092392635
C,-0.1494431188,-5.5070837098,0.0381013461
C,0.6250636441,-5.4076359884,-2.2550154751
C,1.0986469864,-2.4562088214,-1.1461886973
C,2.4539884546,-2.9506959056,-1.1388375673
C,3.2694120951,-1.8703927702,-1.2877383421
C,2.4162622985,-0.7101824433,-1.3774485108
C,2.8756517689,0.5986900133,-1.5851460035
C,4.3343488623,0.7930686342,-1.8574912532
C,4.8966592043,0.3288582368,-3.0584684695
C,6.525999515,1.5963880294,-1.1751083241
C,5.1625168305,1.42997966,-0.9185550928
C,2.0451525266,1.7259622751,-1.5328061388
C,2.5251117936,3.0659988908,-1.7519063888
C,1.492112383,3.906387803,-1.4783543322
C,0.3597417507,3.0927591796,-1.122470517
C,-0.8694673863,3.6823882269,-0.7154149374
C,-0.8938581991,5.1101373606,-0.2891279643
C,-0.0517005863,5.5652504958,0.7418842877
C,-0.9791276127,7.7955787394,0.5363929326
C,-1.8200753001,7.3508506991,-0.4893303653
C,-1.7838021008,6.0150887324,-0.8951624685
C,-2.048506231,2.9538648733,-0.6470329738
C,-3.268353272,3.2000171016,0.0280047129
C,-4.1145134415,2.1053091311,0.0818938351
C,-3.5967656787,0.9452466557,-0.5429431488
H,-6.338282155,0.5216229674,-1.4963347598
H,-8.6275343352,0.0740918722,-0.6652838311
H,-8.9700948236,-1.3761791897,1.3291346643
H,-7.0032519302,-2.3737150385,2.4841524725
H,-4.716176939,-1.9312618534,1.6505924465
H,-4.6385038189,-3.0831325442,-0.9267096088
H,-2.501943132,-4.675751995,-1.2592450341
H,-0.5071402636,-5.0077722014,0.934036353
H,0.8515366437,-4.8322688094,-3.1481352228
H,2.7375963647,-3.9860620462,-1.0254254714
H,4.3483663601,-1.8520911053,-1.3179155871

H,4.2643280115,-0.1620024146,-3.792697477
H,3.524058541,3.3246806262,-2.0679286615
H,1.4810746303,4.9843978773,-1.5329502109
H,-2.5023265259,8.042427683,-0.9747852068
H,-2.4319872726,5.6747878847,-1.6975709987
H,-3.4644233266,4.1369344701,0.5338080554
H,-5.0449072177,2.0910496843,0.6352331727
N,-1.7194322329,-1.4358559986,-0.9151432245
N,1.1007639529,-1.0869250851,-1.2595886892
N,0.7034133292,1.7432980985,-1.188715015
Ni,-0.4139123612,0.0768693314,-1.1064831005
S,-2.1496167104,1.3853246932,-1.4372054331

[S14 (Complete ref. 18)] *Gaussian 16*, Revision C.01, M. J. Frisch, G. W. Trucks, H. B. Schlegel, G. E. Scuseria, M. A. Robb, J. R. Cheeseman, G. Scalmani, V. Barone, G. A. Petersson, H. Nakatsuji, X. Li, M. Caricato, A. V. Marenich, J. Bloino, B. G. Janesko, R. Gomperts, B. Mennucci, H. P. Hratchian, J. V. Ortiz, A. F. Izmaylov, J. L. Sonnenberg, D. Williams-Young, F. Ding, F. Lipparini, F. Egidi, J. Goings, B. Peng, A. Petrone, T. Henderson, D. Ranasinghe, V. G. Zakrzewski, J. Gao, N. Rega, G. Zheng, W. Liang, M. Hada, M. Ehara, K. Toyota, R. Fukuda, J. Hasegawa, M. Ishida, T. Nakajima, Y. Honda, O. Kitao, H. Nakai, T. Vreven, K. Throssell, J. A. Montgomery, Jr., J. E. Peralta, F. Ogliaro, M. J. Bearpark, J. J. Heyd, E. N. Brothers, K. N. Kudin, V. N. Staroverov, T. A. Keith, R. Kobayashi, J. Normand, K. Raghavachari, A. P. Rendell, J. C. Burant, S. S. Iyengar, J. Tomasi, M. Cossi, J. M. Millam, M. Klene, C. Adamo, R. Cammi, J. W. Ochterski, R. L. Martin, K. Morokuma, O. Farkas, J. B. Foresman and D. J. Fox, Gaussian, Inc., Wallingford CT, 2016.

[S15] Z. Chen, C. S. Wannere, C. Corminboeuf, R. Puchta and P. v. R. Schleyer, *Chem. Rev.*, 2005, **105**, 3842–3888.

[S16] R. Herges and D. Geuenich, *J. Phys. Chem. A*, 2001, **105**, 3214–3220.

[S17] Articles for *GAMESS*: (a) M. W. Schmidt, K. K., Baldridge, J. A. Boatz, S. T. Elbert, M. S. Gordon, J. H. Jensen, S. Koseki, N. Matsunaga, K. A. Nguyen, S. J. Su, T. L. Windus, M. Dupuis and J. A. Montgomery, *J. Comput. Chem.*, 1993, **14**, 1347−1363; (b) M. S. Gordon and M. W. Schmidt, in *Theory and Applications of Computational Chemistry: the first forty years*, eds. C. E. Dykstra, G. Frenking, K. S. Kim and G. E. Scuseria, Elsevier, 2005, pp.1167–1189.

[S18] Report for FMO: K. Kitaura, E. Ikeo, T. Asada, T. Nakano and M. Uebayasi, *Chem. Phys. Lett.*, 1999, **313**, 701–706.

[S19] Report for pair interaction energy decomposition analysis (PIEDA): D. G. Fedorov and K. Kitaura, *J. Comput. Chem.*, 2007, **28**, 222–237.

4. Properties of π-electronic cations

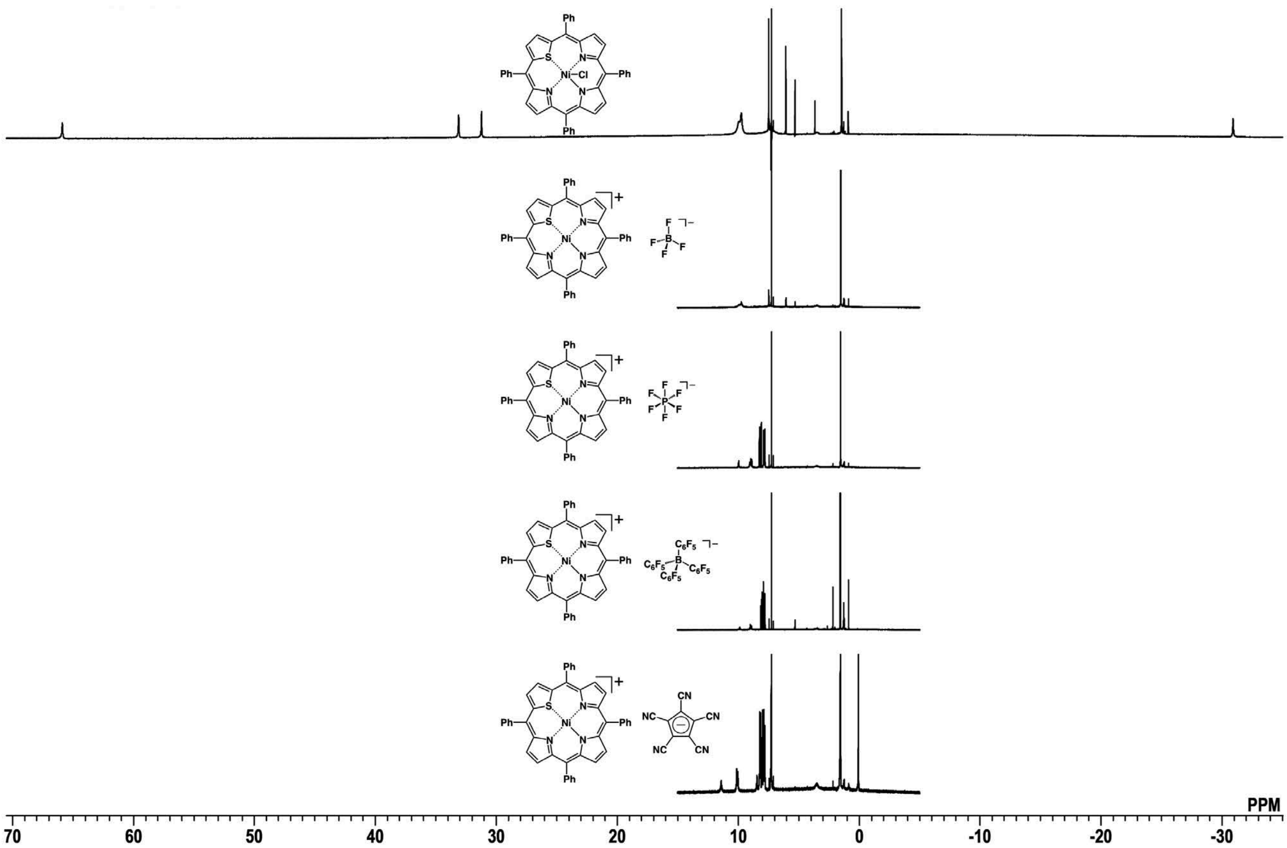

Fig. S42 Summarized ^{1}H NMR spectra of **1ni**$^+$-X$^-$ (X$^-$ = Cl$^-$, BF_4^-, PF_6^-, $B(C_6F_5)_4^-$, PCCp$^-$) in $CDCl_3$ (600 MHz, 20 °C) (Fig. S1–4). The broad signals for **1ni**$^+$-Cl$^-$ in the wide range from 66 to –31 ppm were derived from the paramagnetic Ni^{II} by Cl$^-$ coordination.[S20] The differences in **1ni**$^+$-X$^-$ (X$^-$ = BF_4^-, PF_6^-, $B(C_6F_5)_4^-$, PCCp$^-$) are related with the interactions between the anions and **1ni**$^+$ in solution. The details on the solution-state ion pairing will be examined and reported elsewhere.

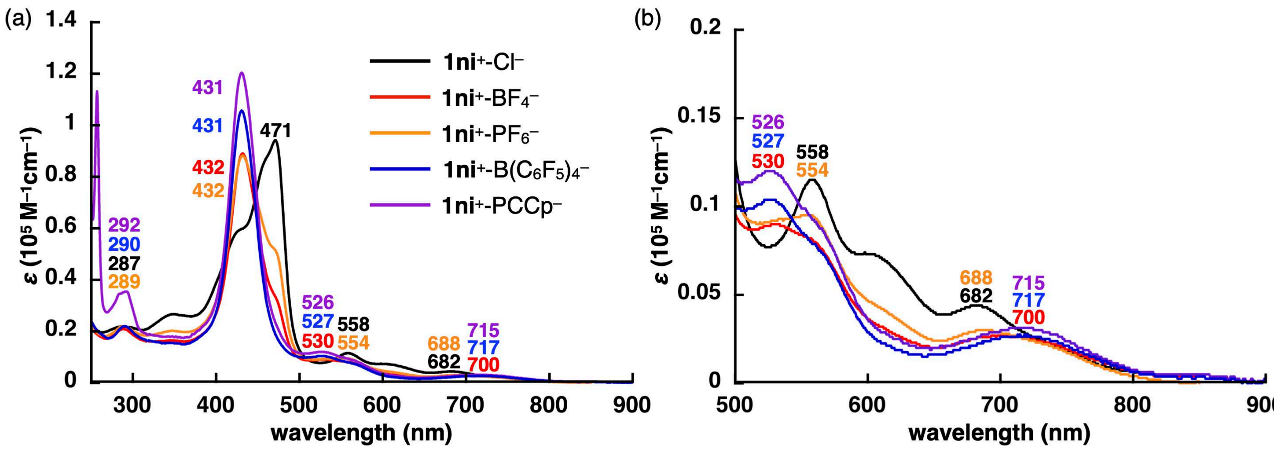

Fig. S43 (a) UV/vis absorption spectra with (b) enlarged version for **1ni**$^+$-X$^-$ (X$^-$ = Cl$^-$, BF_4^-, PF_6^-, $B(C_6F_5)_4^-$, PCCp$^-$) in CH_2Cl_2 (1×10^{-5} M for **1ni**$^+$-Cl$^-$, **1ni**$^+$-BF_4^-, and **1ni**$^+$-PF_6^- and 8×10^{-6} M for **1ni**$^+$-$B(C_6F_5)_4^-$ and **1ni**$^+$-PCCp$^-$). The spectrum of **1ni**$^+$-BF_4^- is similar to that of **1ni**$^+$-Cl$^-$ except for the Soret band, whereas **1ni**$^+$-PF_6^-, **1ni**$^+$-$B(C_6F_5)_4^-$, and **1ni**$^+$-PCCp$^-$ have similar Soret and Q bands. The absence of axial Cl$^-$ coordination resulted in the blue-shifted Soret band at 432 nm for **1ni**$^+$-PF_6^- and at 431 nm for **1ni**$^+$$B(C_6F_5)_4^-$ and **1ni**$^+$-PCCp$^-$ compared to that of **1ni**$^+$-Cl$^-$ at 471 nm.

[S20] J. Lisowski, L. Latos-Grażyński and L. Szterenberg, *Inorg. Chem.*, 1992, **31**, 1933–1940.